Identification and characterization of a novel anti-inflammatory lipid isolated from Mycobacterium vaccae, a soil-derived bacterium with immunoregulatory and stress resilience properties

Smith, David G; Martinelli, Roberta; Besra, Gurdyal S; Illarionov, Petr A; Szatmari, Istvan; Brazda, Peter; Allen, Mary A; Xu, Wenqing; Wang, Xiang; Nagy, László; Dowell, Robin D; Rook, Graham A W; Rosa Brunet, Laura; Lowry, Christopher A

DOI:
10.1007/s00213-019-05253-9

Document Version
Peer reviewed version

Citation for published version (Harvard):
Smith, DG, Martinelli, R, Besra, GS, Illarionov, PA, Szatmari, I, Brazda, P, Allen, MA, Xu, W, Wang, X, Nagy, L, Dowell, RD, Rook, GAW, Rosa Brunet, L & Lowry, CA 2019, 'Identification and characterization of a novel anti-inflammatory lipid isolated from Mycobacterium vaccae, a soil-derived bacterium with immunoregulatory and stress resilience properties', *Psychopharmacology*, vol. 236, no. 5, pp. 1653-1670. https://doi.org/10.1007/s00213-019-05253-9

Identification and characterization of a novel anti-inflammatory lipid isolated from *Mycobacterium vaccae*, a soil-derived bacterium with immunoregulatory and stress resilience properties

DAVID G. SMITH[a]#*, ROBERTA MARTINELLI[b]†, GURDYAL S. BESRA[c], PETR A. ILLARIONOV[c], ISTVAN SZATMARI[d], PETER BRAZDA[d], MARY A. ALLEN[e,f], WENQING XU[a], XIANG WANG[a], LÁSZLÓ NAGY[d,g]Ϧ, ROBIN D. DOWELL[e,f], GRAHAM A.W. ROOK[b], LAURA ROSA BRUNET[b], CHRISTOPHER A. LOWRY[h,i,]#

[a]Department of Chemistry and Biochemistry, University of Colorado Boulder, Boulder, CO 80309, USA

[b]Center for Clinical Microbiology, UCL (University College London), London WC1E 6BT, United Kingdom

[c]School of Bioscience, University of Birmingham, Edgbeston, Birmingham B15 2TT, United Kingdom

[d]Department of Biochemistry and Molecular Biology, Faculty of Medicine, University of Debrecen, Egyetem tér, 1, H-4032, Debrecen, Hungary

[e]Molecular, Cellular, and Developmental Biology, University of Colorado Boulder, Boulder, CO 80309, USA

[f]BioFrontiers Institute, University of Colorado Boulder, Boulder, CO 80303, USA

[g]MTA-DE "Lendület" Immunogenomics Research Group, University of Debrecen, Egyetem tér, 1, H-4012, Debrecen, Hungary

[h]Department of Integrative Physiology, Center for Neuroscience, and Center for Microbial Exploration, University of Colorado Boulder, Boulder, CO 80309, USA

[i]Senior Fellow, inVIVO Planetary Health, of the Worldwide Universities Network (WUN), West New York, NJ 07093, USA

*Current address, Department of Pathology, Anatomy, and Cellular Biology, Thomas Jefferson University, Philadelphia, PA 19107, USA

†Current address, Department of Medicine, Beth Israel Deaconess Medical Center, Harvard Medical School, Boston, MA 02215, USA

[ϑℓ]Department of Medicine, Johns Hopkins University, Johns Hopkins All Children's Hospital, Saint Petersburg, FL 33701, USA

#Corresponding authors and lead contacts

Email: christopher.lowry@colorado.edu

Email: david.smith3@jefferson.edu

Co-author emails:

DAVID G. SMITH, david.smith3@jefferson.edu

ROBERTA MARTINELLI, roberta.martinelli@merck.com

GURDYAL S. BESRA, G.Besra@bham.ac.uk

PETR A. ILLARIONOV, illar@yahoo.com

ISTAN SZATMARI, szatmari@med.unideb.hu

PETER BRAZDA, p.brazda@science.ru.nl

MARY A. ALLEN, Mary.A.Allen@colorado.edu

WENQING XU,wenqing.xu@colorado.edu

XIANG WANG,xiang.wang@colorado.edu

LÁSZLÓ NAGY, lnagy@jhmi.edu

ROBIN D. DOWELL, Robin.Dowell@colorado.edu

GRAHAM A.W. ROOK, g.rook@ucl.ac.uk

LAURA ROSA BRUNET, laura@rosabrunetconsulting.co.uk

CHRISTOPHER A. LOWRY, christopher.lowry@colorado.edu

ACKNOWLEDGEMENTS

We are grateful to Zachary D. Barger for proof reading the manuscript. This work was supported by the National Institute of Mental Health (grant number 1R21MH116263; CAL). Dr. Christopher A. Lowry is supported by the Department of the Navy, Office of Naval Research Multidisciplinary University Research Initiative (MURI) Award (grant number N00014-15-1-2809), Department of Veterans Affairs Office of Research and Development (VA-ORD) RR&D Small Projects in Rehabilitation Research (SPiRE) (I21) (grant number 1 I21 RX002232-01), Colorado Clinical & Translational Sciences Institute (CCTSI) Center for Neuroscience (grant number CNSTT-15-145), the Colorado Department of Public Health and Environment (CDPHE; grant number DCEED-3510), and the Alfred P. Sloan Foundation (grant number, G-2016-7077).

Dr. Robin Dowell is supported by NSF Career MCB #1350915. We thank the University of Colorado Boulder BioFrontiers Institute Next-Gen Sequencing Core Facility, which performed the Illumina sequencing.

CONFLICTS OF INTEREST

Christopher A. Lowry serves on the Scientific Advisory Board of Immodulon Therapeutics Ltd. Dr. Robin Dowell is a founder and scientific advisor of Arpeggio Biosciences.

ABSTRACT

Mycobacterium vaccae (NCTC 11659) is an environmental saprophytic bacterium with anti-inflammatory, immunoregulatory, and stress resilience properties. Previous studies have shown that whole, heat-killed preparations of *M. vaccae* prevent allergic airway inflammation in a murine model of allergic asthma. Recent studies also demonstrate that immunization with *M. vaccae* prevents stress-induced exaggeration of proinflammatory cytokine secretion from mesenteric lymph node cells stimulated *ex vivo*, prevents stress-induced exaggeration of chemically-induced colitis in a model of inflammatory bowel disease, and prevents stress-induced anxiety-like defensive behavioral responses. Furthermore, immunization with *M. vaccae* induces anti-inflammatory responses in brain, and prevents stress-induced exaggeration of microglial priming. However, the molecular mechanisms underlying anti-inflammatory effects of *M. vaccae* are not known. We have purified and identified a unique anti-inflammatory triglyceride, 1,2,3-tri[*Z*-10-hexadecenoyl]glycerol, from *M. vaccae* and evaluated its effects in freshly isolated murine peritoneal macrophages. The free fatty acid form of 1,2,3-tri[*Z*-10-hexadecenoyl]glycerol, 10(*Z*)-hexadecenoic acid, decreased lipopolysaccharide-stimulated secretion of the proinflammatory cytokine IL-6 *ex vivo*. Meanwhile, next generation mRNA sequencing revealed that pretreatment with 10(*Z*)-hexadecenoic acid upregulated genes associated with peroxisome proliferator-activated receptor alpha (PPARα) signaling in lipopolysaccharide-stimulated macrophages, in association with a broad transcriptional repression of inflammatory markers. We confirmed using luciferase-based transfection assays that 10(*Z*)-hexadecenoic acid activated PPARα signaling, but not PPARγ, PPARδ, or retinoic acid receptor (RAR) α signaling. The effects of 10(*Z*)-hexadecenoic acid on lipopolysaccharide-stimulated secretion of IL-6 were prevented by PPARα antagonists and absent in PPARα-

deficient mice. Future studies should evaluate the effects of 10(*Z*)-hexadecenoic acid on stress-induced exaggeration of peripheral inflammatory signaling, central neuroinflammatory signaling, and anxiety- and fear-related defensive behavioral responses.

KEYWORDS

10(*Z*)-hexadecenoic acid, bacteria, inflammation, interleukin 6, lipid, macrophage, mycobacteria, PPAR, RNAseq, *vaccae*

ABBREVIATIONS

CD, cluster of differentiation
CNS, central nervous system
DC, dendritic cell
DSM-5, Diagnostic and Statistical Manual of Mental Disorders (5th ed.).
IL, interleukin
IFN, interferon
IRF, interferon regulatory factor
LPS, lipopolysaccharide
MGB, microbiota–gut–brain
NCTC, National Collection of Type Cultures
NF-κB, nuclear factor kappa-light-chain-enhancer of activated B cells
PEA, palmitoylethanolamide
PPAR, peroxisome proliferator-activated receptor
PTSD, posttraumatic stress disorder
RAR, retinoic acid receptor
TGFβ, transforming growth factor beta
TLR, toll-like receptor
Treg, regulatory T cell

INTRODUCTION

The global prevalence of anxiety disorders has been estimated to be 7.3%, ranging from 5.3% in African cultures to 10.4% in Euro/Anglo cultures (Baxter et al. 2013). According to the Diagnostic and Statistical Manual of Mental Disorders (5th ed.) (DSM-5; (American Psychiatric Association 2013)), anxiety disorders include those that share features of excessive fear and anxiety and related behavioral disturbances, such as generalized anxiety disorder, panic disorder, social anxiety disorder (social phobia), and specific phobia (American Psychiatric Association 2013). Posttraumatic stress disorder (PTSD), although formerly classified as an anxiety disorder, is classified as a trauma- and stressor-related disorder (APA, 2013). Collectively, anxiety and trauma-related disorders are complex and multifactorial, and their differentiation and management are complicated by phenotypic heterogeneity. The etiology and pathophysiology of these disorders are thought to involve interactions among the genome, epigenome, and environment (Nugent et al. 2011). Recently, investigation of the etiology and pathophysiology of psychiatric and neurological diseases has expanded to include a potential role of the microbiota–gut–brain (MGB) axis (Forsythe et al. 2010; Cryan and Dinan 2012, 2015; Leclercq et al. 2016). Of particular interest, evidence from preclinical and clinical studies suggests that exaggerated inflammation, which in some cases may be secondary to dysregulation of the microbiome, may be a risk factor for the development of trauma- and stressor-related disorders (for review, see (Langgartner et al. 2018)). These studies raise the question of whether or not microbial-based interventions with anti-inflammatory or immunoregulatory properties may have value in the prevention or treatment of trauma- and stressor-related disorders.

Evidence suggests that some common pathogenic and non-pathogenic microorganisms, to which humans have been exposed throughout evolution, drive anti-inflammatory and

immunoregulatory mechanisms that inhibit inappropriate immune responses by the host (Rook and Rosa Brunet 2002; Rook 2009, 2010; Okada et al. 2010). Throughout human evolution, the interactions between these ancestral microorganisms, which we have collectively referred to as "Old Friends", and the innate immune system promoted immunoregulation. These "Old Friends" included microorganisms that: 1) were part of host physiology (human microbiota); 2) were harmless but inevitably contaminating air, food and water (environmental microbiota); or 3) led to severe host tissue damage when attacked by the host immune system (e.g., helminthic parasites) (Rook 2013; Blaser 2017).

"Old Friends" are thought to suppress host inflammation through a variety of mechanisms, including the induction of specific subsets of antigen-presenting cells such as macrophages and dendritic cells (DCs) and modulation of innate immunity (Le Bert et al. 2011; Garn et al. 2016; Lowry et al. 2016). In their absence, the host may develop inappropriate immune responses to allergens, self-antigens, or gut microbiota. It has been hypothesized that increases in allergies, autoimmune diseases, inflammatory bowel diseases, and psychiatric disorders in modern living conditions may be due, in part, to decreased exposure to "Old Friends" (Rook 2010; Lyte and Cryan 2014; Bloomfield et al. 2016; Lowry et al. 2016; Stamper et al. 2016). In parallel, individuals with a diagnosis of PTSD have a higher risk of development of any autoimmune disease, relative to those with other psychiatric disorders, or relative to those with no psychiatric disorder (O'Donovan et al. 2015), suggesting that impaired immunoregulation or inappropriate inflammation may confer risk for development of both autoimmune conditions and PTSD. The saprophytic mycobacterium, *Mycobacterium vaccae* (National Collection of Type Cultures (NCTC) 11659), has shown encouraging therapeutic potential in diseases of inflammation and immunodysregulation (Gutzwiller et al. 2007; Rook et al. 2007), and has shown

immunoregulatory and stress-protective effects in murine models (Zuany-Amorim et al. 2002; Adams et al. 2004; Lowry et al. 2007; Reber et al. 2016; Fox et al. 2017; Frank et al. 2018). Mycobacteria are abundant in municipal water supplies (Gebert et al. 2018) and are a normal component of the healthy human microbiome of the oral cavity (buccal mucosa and dental plaque) and upper respiratory tract (nostrils and oropharynx), and therefore are considered part of the microbiome of the upper airways (Macovei et al. 2015).

The identification of specific microbially-derived molecules with anti-inflammatory or immunoregulatory properties may provide novel therapeutic avenues for the treatment of diseases of immunodysregulation, or trauma- and stressor-related disorders where exaggerated inflammation is thought to be a risk factor (Lowry et al. 2016; Langgartner et al. 2018). We have previously shown that treatment with a heat-killed preparation of the saprophytic mycobacterium, *M. vaccae*, prevents murine allergic pulmonary inflammation by inducing $CD4^{+}CD45RB^{low}$ Tregs (Zuany-Amorim et al. 2002). These cells are allergen-specific and upon passive transfer can protect recipient allergic mice from airway inflammation by significantly reducing eosinophilia in the lungs. In addition, treatment with *M. vaccae* induces a population of pulmonary $CD11c^{+}$ antigen-presenting cells, which are characterized by increased expression of IL-10, transforming growth factor beta (TGFβ) and interferon α (IFNα) (Adams et al. 2004). Furthermore, at least *in vitro*, priming of human DCs with *M. vaccae* induces strong inhibition of Th2 responses (Le Bert et al. 2011).

Meanwhile, we've shown that immunization of mice with *M. vaccae* promotes a more proactive response to a chronic psychosocial stressor, prevents stress-induced colitis, prevents stress-induced exaggeration of chemically-induced colitis in a model of inflammatory bowel disease, and attenuates anxiety-like defensive behavioral responses (Reber et al. 2016). Consistent with

these findings, immunization with *M. vaccae* prevents stress-induced exaggeration of interferon gamma and IL-6 secretion from freshly isolated mesenteric lymph node cells stimulated with anti-CD3/anti-CD28 *ex vivo*. Importantly, preimmunization with *M. vaccae*, in stressed mice, resulted in a two orders of magnitude increase in IL-10 secretion from mesenteric lymph node cells stimulated *ex vivo*. However, until now, specific constituents of *M. vaccae* that suppress inflammation in macrophages in the periphery or central nervous system have not been identified.

Through a screening process of *M. vaccae* NCTC 11659 lipid extracts, a single triglyceride, 1,2,3-tri[*Z*-10-hexadecenoyl]glycerol, was identified with potential immunotherapeutic benefits (Rosa Brunet and Rook 2008). The lipid was demonstrated to prevent allergic airway inflammation, and the lipid recapitulated the therapeutic effects of whole heat-killed *M. vaccae*. The protective phenotype was characterized by increased IL-10, decreased IL-5, and reduced infiltration of eosinophils and macrophages in bronchoalveolar lavage fluid (Rosa Brunet and Rook 2008). It was also shown that the efficacy of the triglyceride was not dependent on the glycerol structure, as the synthetic, constituent free fatty acid, 10(*Z*)-hexadecenoic acid, was sufficient to suppress pulmonary airway inflammation. The mechanism through which this long-chain, monounsaturated fatty acid was capable of limiting symptoms of inflammation is unknown, but it is explored here in a model of macrophage activation.

Notably, it is relatively rare in nature for an organism to naturally produce a fatty acid that is unsaturated at the C10 position, yet several mycobacteria species—including *M. vaccae*, can perform that desaturation (Scheuerbrandt and Bloch 1962; Coyle et al. 1992; Böttger et al. 1993; Springer et al. 1993; Suutari and Laakso 1993; Chou et al. 1998; Tay et al. 1998; Pacífico et al. 2018). We successfully synthesized the free fatty acid, 10(*Z*)-hexadecenoic acid, and using cell-

based assays and RNA-seq, revealed that 10(*Z*)-hexadecenoic acid upregulated genes associated with the peroxisome proliferator-activated receptor (PPAR) signaling pathway and inhibited proinflammatory signaling of activated macrophages *ex vivo*. Furthermore, studies using cultured cells transfected with lipid-regulated transcription factors revealed that both the monoacylglycerol lipid constituent of *M. vaccae* and its free fatty acid form selectively increased PPARα signaling. The effects of 10(*Z*)-hexadecenoic acid to inhibit proinflammatory signaling of activated macrophages *ex vivo* were prevented by PPARα antagonists and absent in PPARα-deficient mice. This is the first report, to our knowledge, to show that a synthetic *M. vaccae*-derived lipid acts to induce anti-inflammatory responses in host immune cells by acting as an agonist at host PPARα receptors.

MATERIALS AND METHODS

Animals

Adult male BALB/c mice (BALB/cAnHsd; Cat. No. 047; Harlan, Indianapolis, IN, USA), 6-8 weeks old, were used and housed under standard conditions with food and water available *ad libitum*. Adult male PPARα$^{-/-}$ (B6;129S4-*Ppara*^{tm1Gonz}/J; Cat. No. 008154; Jackson Laboratories, Bar Harbor, ME, USA) and control mice (C57BL/6J; Cat. No. 000664; Jackson Laboratories), 6-8 weeks old, were used and housed under standard conditions with food and water available *ad libitum*. Although the C57BL/6J inbred strain is considered an approximate control for the PPARα$^{-/-}$ mice (B6;129S4-*Ppara*^{tm1Gonz}/J; Jackson Laboratories) future studies should ideally compare PPARα$^{-/-}$ mice to wild type littermates.

All experimental protocols were consistent with the National Institutes of Health *Guide for the Care and Use of Laboratory Animals*, Eighth Edition (The National Academies Press, 2011) and

231 the Institutional Animal Care and Use Committee at the University of Colorado Boulder
232 approved all procedures. This work was covered under CU Boulder IACUC Protocol Numbers
233 2134-14MAY2018 and 2361-14MAY2018-DT. The research described here was conducted in
234 compliance with The ARRIVE Guidelines: Animal research: reporting of in vivo experiments,
235 originally published in PLOS Biology, June 2010 (Kilkenny and Altman 2010). All possible
236 efforts were made to minimize the number of animals used and their suffering.

237 **Synthesis of 10(*Z*)-hexadecenoic acid; (10*Z*)-hexadec-10-enoic acid (CAS No. 2511-97-9)**

238 Unless otherwise noted, reagents were obtained commercially and used without further
239 purification. Dichloromethane (CH_2Cl_2) was distilled over calcium hydride (CaH_2) under a
240 nitrogen atmosphere. Tetrahydrofuran (THF; $(CH_2)_4O$) was distilled from sodium-benzophenone
241 under a nitrogen atmosphere. Thin-layer chromatography analysis of reaction mixtures was
242 performed on Dynamic Adsorbents, Inc., silica gel F-254 TLC plates. Flash chromatography was
243 carried out on Zeoprep 60 ECO silica gel. ^1H spectra were recorded with a Varian INOVA 500
244 spectrometer. Compounds were detected by monitoring UV absorbance at 254 nm.

245 To a 5 mL sealed tube containing 1-heptene (0.50 mL, 3.55 mmol), methyl 10-undecenoate
246 (0.080 mL, 0.36 mmol) and 0.35 mL THF was added to a Grubbs Z-selective metathesis catalyst
247 (2.2 mg, 3.48 µmol, Cat. No. 771082, Sigma-Aldrich, St. Louis, MO, USA). The reaction was
248 stirred at 45 ^oC for 8 h before cooling to room temperature. The slurry was filtrated through a
249 short plug of silica gel and concentrated. The obtained oil was dissolved in 1.0 mL THF. The
250 solution was cooled to 0 ^oC, then 9-borabicyclo[3.3.1]nonane (9-BBN) solution in THF (1.28
251 mL, 0.50 M, 0.64 mmol) was added. After 2 h stirring at 0 ^oC, the reaction was quenched with 60
252 µL EtOH, then 1.5 mL pH 7 potassium phosphate buffer and 1.5 mL 30% H_2O_2. The mixture
253 was stirred at room temperature for 12 h, then extracted with 5 mL EtOAc three times. The

combined organic layers were washed with 4 mL saturated $Na_2S_2O_3$ and 3 mL brine, then dried over Na_2SO_4, filtered and concentrated. To the crude oil in 1.0 mL THF was added LiOH monohydrate (38 mg, 0.90 mmol) in 1.0 mL water. After 2 h, the reaction solution was cooled to 0 ^oC before addition of 0.91 mL 1.0 N HCl. After being concentrated under reduced pressure, the aqueous solution was saturated with NaCl and extracted with 3 mL dichloromethane three times. The combined organic layers were dried over Na_2SO_4, filtered and concentrated. Purification by flash chromatography (2:1:1 hexanes/dichloromethane/diethyl ether) provided (10*Z*)-hexadec-10-enoic acid (0.022 g, 90%) as a colorless oil. ^1H NMR (500 MHz, $CDCl_3$): δ 5.48 – 5.22 (m, 2H), 2.35 (t, J = 7.5 Hz, 2H), 2.01 (q, J = 6.6 Hz, 4H), 1.63 (p, J = 7.4 Hz, 2H), 1.35 – 1.15 (m, 16H), 0.88 (t, J = 6.9 Hz, 3H).

Murine peritoneal macrophage isolation and screening

Murine peritoneal macrophages were isolated and cultured as previously described (Zhang et al. 2008) and used to determine the effects of 10(*Z*)-hexadecenoic acid on lipopolysaccharide-induced IL-6 secretion. Briefly, mice received a single injection of 3% thioglycollate medium (1 mL, i.p.; Cat. No. 9000-294, VWR, Radnor, PA, USA). Mice were euthanized 96 h later using cervical dislocation, and macrophages were collected in Dulbecco's phosphate-buffered saline (DPBS; Cat. No. 14190136, Invitrogen, Carlsbad, CA, USA). Cells were centrifuged and resuspended in Dulbecco's Modified Eagle Medium/Nutrient Mixture F-12 (DMEM/F-12; Cat. No. 10565018, Invitrogen) supplemented to be 10% (v/v) fetal bovine serum (Cat. No. 16000036, Invitrogen) and 1% penicillin/streptomycin (Cat. No. 15140148, Invitrogen). One mouse yielded enough cells for one experimental replicate. 1 x 10^5 cells/well were allowed to adhere for 1.5 h before being washed with DPBS. 10(*Z*)-hexadecenoic acid was dissolved in DMEM/F-12 with 0.5% (v/v) dimethyl sulfoxide (Cat. No. D8418, Sigma-Aldrich). The

macrophages were incubated with either 10(*Z*)-hexadecenoic acid (0.4 µM, 4 µM, 20 µM, 100 µM, 500 µM, 1000 µM) or DMEM/F-12 for 1 h before being stimulated with either 1 µg/ml lipopolysaccharide (serotype 0127:B8, Sigma-Aldrich, St. Louis, MO, USA) or DMEM/F-12. Culture supernatants were collected at 6, 12, and 24 h post-stimulation.

Cytokine measurements

Cell culture supernatants (10 µl) from freshly isolated peritoneal macrophages were diluted 1:200, and IL-6 was measured using ELISA (Cat. No. 431304, BioLegend, San Diego, CA, USA). The assay has a minimal detectable concentration of 2 pg/ml IL-6. All samples were measured using duplicate wells in the ELISA.

Cytotoxicity assay

Cytotoxicity was determined using the sulforhodamine B (SRB) colorimetric assay, as previously described (Vichai and Kirtikara 2006). Briefly, without removing the culture media, cells were fixed by adding cold trichloroacetic acid and incubated at 4 °C for 1 h. The plates were washed with slow-running tap water and set out to dry overnight. Then, 0.057% SRB (Cat. No. AC333130050, Fisher, Pittsburgh, PA, USA), solubilized in 10 mM Tris (Cat. No. BP153, Fisher), was added to each well. After 30 min, plates were washed with 1% acetic acid and set out to dry overnight. SRB was measured at 490 nm on a Synergy HT microplate reader (Part Number 7091000, Biotek, Winooski, VT, USA). Cell viability was expressed as the ratio of experimental and control growth.

Ligands

For studies using reporter gene assays following transfection of COS1 cells, rosiglitazone, troglitazone, and WY14643 were obtained from Alexis Biochemicals (San Diego, CA, USA);

ATRA and AM580 were obtained from Sigma-Aldrich. In addition, GW9662 was a gift from T.M. Willson (GlaxoSmithKline, Brentford, United Kingdom). For experiments using freshly isolated peritoneal macrophages, GW 6471 (Cat. No. 4618), GW 9662 (Cat. No. 1508), GSK 0660 (Cat. No. 3433), WY 14643 (Cat. No. 1312), rosiglitazone (Cat. No. 5325), GW 0742 (Cat. No. 2229) were obtained from Tocris Bioscience (Bristol, United Kingdom).

Transfections and reporter gene assays

Cells were transfected with the following receptor and reporter constructs: Gal4-PPARα-LBD, Gal4-PPARγ-LBD, Gal4-PPARδ-LBD, Gal4-RARα-LBD, pMH100-TK-luc, and pCMX-β-galactosidase (Chen and Evans 1995). All transfection experiments were performed with COS1 cells using polyethylenimine (Sigma-Aldrich) reagent (Szatmari et al. 2006). After 6–8 h of the transfection, the medium was replaced with DMEM medium containing the indicated ligands or vehicle (as control) (Chen and Evans 1995; Benko et al. 2003). Cells were lysed and assayed for reporter expression 18 h after transfection. The luciferase assay system (Promega, Madison, WI, USA) was used as described previously (Nagy et al. 1999). Measurements were carried out with a Wallac Victor-2, multilabel counter. Luciferase activity of each sample was normalized to the β-galactosidase activity.

RNA extraction and library preparation

Total RNA content of 1 x 10^5 macrophages pretreated for 1 h with 200 μM 10(*Z*)-hexadecenoic acid (utilizing separate macrophage preparations from $n = 3$ mice) or vehicle (utilizing separate macrophage preparations from $n = 3$ mice) and stimulated with 1 μg/ml LPS was extracted using TRI Reagent® (Cat. No. T9424, Sigma-Aldrich) according to manufacturer's instructions. The RNA input was quantified on a Qubit™ 3.0 Fluorometer (Cat. No. Q33216, Thermo Fisher, Waltham, MA, USA) to ensure there was sufficient starting material. The RNA sequencing

libraries were generated with the NEBNext rRNA Depletion Kit (Cat. No. E6310, New England BioLabs) in order to enrich the samples in mRNA, and NEBNext Ultra Directional RNA Library Prep Kit for Illumina (Cat. No. 7240, New England BioLabs). Briefly, mRNA was purified from 100 ng of total RNA, fragmented, and converted to double stranded cDNA. Barcodes were ligated to the cDNA fragments, and prior to PCR enrichment of the library, the cDNA product was quantified on a Qubit 3.0 Fluorometer (Thermo Fisher). The integrity of the purified oligo libraries was evaluated on an Agilent Bioanalyzer 2100 (Cat. No. G2939BA, Agilent, Santa Clara, CA, USA).

Sequencing

Libraries were sequenced at the Next Generation Sequencing Facility at the University of Colorado Boulder. The libraries were multiplexed and sequenced on an Illumina HiSeq 2000 Sequencing System (Cat. No. SY-401-1001, Illumina, San Diego, CA, USA). For each sample, paired-end 100-bp reads were sequenced using V3 chemistry.

RNA read processing, mapping, and differential expression

Quality analysis of sequencing data was done using FastQC. The adaptors and low quality raw reads were cut with Trimmomatic (version 0.32) (Bolger et al. 2014). The reads were aligned to the mouse genome, mm10 (University of California, Santa Cruz, CA, USA), using the TopHat2 sequence aligner (version 2.0.6) (Kim et al. 2013). Reads mapping to exon features were counted using HTseq (version 0.6.1) (Anders et al. 2015). The raw reads and count data have been deposited in the GEO database under accession number GSE125930. Differentially expressed genes were identified using the R package, DESeq (version 1.28.0) (Anders and Huber 2010).

Statistical analysis

Data are presented as means ± SEM or means + SEM. Data were subjected to a normality test and one-way analysis of variance (ANOVA); Fisher's least significant difference (LSD) tests were performed as appropriate. A two-tailed p value ≤ 0.05 was considered significant. ELISA IL-6 data were analyzed using linear mixed effects models using the software package SPSS (version 21.0, SPSS Inc., Chicago, IL, USA). Network visualizations were created in Cytoscape (version 3.5.1) using an enrichment map plug-in (Merico et al. 2011).

RESULTS

10(*Z*)-hexadecenoic acid decreases LPS-induced secretion of IL-6 in macrophages

To simulate inflammation, freshly isolated mouse peritoneal macrophages were challenged with LPS (1 µg/mL) *ex vivo* (outlined in Fig. 1). Macrophages that were cultured in the presence of 10(*Z*)-hexadecenoic acid (0.4 µM, 4 µM, 20 µM, 100 µM, 500 µM, 1000 µM) for 1 h prior to 1 µg/mL LPS stimulation secreted less IL-6 relative to macrophages cultured with media alone prior to LPS stimulation (Fig. 2A-C) ($F_{(1,111)} = 15.20$, $p < 0.001$). This difference was observable as early as 6 h after LPS challenge, and was sustained for at least 24 h. We selected the 6 h, 12 h, and 24 h time points for measurement of IL-6 as previous studies have shown increased IL-6 secretion using LPS-stimulated peritoneal macrophage cultures in mice at these time points, with linear increases in IL-6 up to the 24 h time point (Shacter et al. 1993; Wollenberg et al. 1993; Lin and Tang 2007; Lee et al. 2015; Arteaga Figueroa et al. 2017). The effect also appeared to be concentration and time dependent. The lowest concentration of 10(*Z*)-hexadecenoic acid (0.4 µM) was ineffective at 6 h, but reduced IL-6 secretion to 40% of control levels at 24 h. Using a constrained logistic model on the relative secretion of IL-6, we estimated the EC50 to be 823 µM, 115 µM, and 190 µM at the 6h, 12h, and, 24h observations, respectively (Fig. 2). Post hoc pairwise comparisons of raw IL-6 values relative to paired media control values at the same time

point (n = 3 per group) are presented in Table S1. This time and concentration dependence may indicate that a receptor-mediated transcriptional change is occurring. In contrast to the effects of 10(*Z*)-hexadecenoic acid on LPS-induced IL-6 secretion, it had no detectable effect on IL-6 secretion by itself (IL-6 was undetectable in all conditions; Fig. S1). We cannot exclude the possibility, however, that 10(*Z*)-hexadecenoic acid by itself had effects on IL-6 secretion that were below the limit of detectability of the assay used (i.e., 2 pg/mL). Cell viability was measured to dispel the possibility that senescence or cell death was contributing to reduced IL-6 secretion. Using a high concentration (1 mM) of 10(*Z*)-hexadecenoic acid, less than 40% of macrophages were viable at most time points. However, macrophages cultured with all other concentrations of 10(*Z*)-hexadecenoic acid studied (0.4 µM, 4 µM, 20 µM, 100 µM, 500 µM) were as viable as media controls (Fig. S2).

Treatment with 10(*Z*)-hexadecenoic acid induces a broad anti-inflammatory transcriptional profile in LPS-stimulated macrophages

To explore the potential effects of 10(*Z*)-hexadecenoic acid on transcriptional responses in LPS-stimulated macrophages, we used RNA-seq. Murine peritoneal macrophages were incubated with 200 µM 10(*Z*)-hexadecenoic acid for 1 h prior to stimulation with LPS. Using IL-6 as a measure for the suppressive activity of 10(*Z*)-hexadecenoic acid, we estimated the EC_{50} at 12h to be 115 µM. The 200 µM concentration was chosen as it was sufficiently larger than the EC_{50}, but less than a concentration that would affect macrophage viability. After 12 h, the RNA was extracted and depleted of rRNA. We selected the 12 h time point for measurement of mRNA using RNAseq as previous studies have shown increased IL-6 secretion using LPS-stimulated peritoneal macrophage cultures in mice at this time point, as well as the ability to suppress IL-6 mRNA expression at this time point by interfering with a TLR4-MyD88-BLT2-Nox1-ROS-NF-

κB pathway leading to IL-6 secretion (Lee et al. 2015). The cDNA libraries were sequenced in a 100bp paired-end experiment generating 51-63 million reads per sample (Table S2; Fig. S3).

For differential expression, we examined LPS-stimulated macrophages pretreated with either 10(*Z*)-hexadecenoic acid or vehicle (GSE125930). Differentially expressed transcripts were identified using the R package, DESeq (Anders and Huber 2010). A total of 203 genes were found to be differentially expressed with an FDR-adjusted $p < 0.1$ (Table S3). Of the 203 differentially expressed genes, 109 were downregulated in the 10(*Z*)-hexadecenoic acid condition, and 20% of those genes were associated with proinflammatory processes (Table S4). The top 20 differentially expressed genes are reported in Fig. 3A. Consistent with the *ex vivo* macrophage experiments measuring IL-6 protein with ELISA, the second most significantly differentially expressed transcript was IL-6 (Table S3).

PPARα regulated genes are associated with 10(Z)-hexadecenoic acid treatment in LPS-stimulated macrophages

To better understand the pathways affected by 10(*Z*)-hexadecenoic acid treatment, the list of 203 differentially expressed genes were queried against the Database for Annotation, Visualization and Integrated Discovery (DAVID) (Huang et al. 2009). Within the top 40 most significantly enriched KEGG pathways, 34 (i.e., 85%) were related to disease or inflammation (Table S5). In addition, 32 of the top 40 most significantly enriched KEGG pathways (i.e., 82%) were exclusively enriched for genes that were significantly downregulated by treatment with 10(*Z*)-hexadecenoic acid. Among these most significantly affected pathways, there was a wide scope of immunological context, which included infections, diseases, cytokine signaling, and various inflammatory pathways. The top 5 pathways with genes that were exclusively downregulated by treatment with 10(*Z*)-hexadecenoic acid are reported in Fig. 3C.

While the majority of pathways with genes affected by 10(*Z*)-hexadecenoic acid involved genes that were exclusively downregulated by 10(*Z*)-hexadecenoic acid, some pathways involved genes that were exclusively upregulated by 10(*Z*)-hexadecenoic acid. Of the top 40 pathways, 7 (i.e., 17.5%) pathways were exclusively enriched for genes that were significantly upregulated by treatment with 10(*Z*)-hexadecenoic acid. Overall, of 203 genes that were differentially expressed following treatment with 10(Z)-hexadecenoic acid, 93 genes (46%) were upregulated. The pathways with detectable enrichment involved regulation of lipolysis in adipocytes, glycerolipid metabolism, circadian entrainment, PPAR signaling pathway, and extracellular matrix-receptor interaction (Fig. 3B). The top 5 pathways with genes that were exclusively upregulated by treatment with 10(*Z*)-hexadecenoic acid are reported in Fig. 3B. The PPAR signaling pathway was among the top 5 most-enriched KEGG pathways with genes that were exclusively upregulated by treatment with 10(*Z*)-hexadecenoic acid (Fig. 3B).

In a secondary analysis, rather than rely on a subset of genes for biological interpretation, we used all expression data in Gene Set Enrichment Analysis (GSEA). We queried all detected transcripts against the KEGG pathways database (c2.cp.kegg.v6.2), and the top 5 enriched gene sets for the 10(*Z*)-hexadecenoic acid phenotype were: “peroxisome” (KEGG: hsa04146), a main site of fatty acid oxidation via the β-oxidation cycle, “ppar_signaling_pathway” (KEGG: hsa03320), “citrate_cycle_tca_cycle” (KEGG: hsa00020), “fatty_acid_metabolism” (KEGG: hsa00071), and “propanoate_metabolism” (KEGG: hsa00640) (Table S6). Of potential interest, four of these KEGG pathways, “peroxisome” (KEGG: hsa04146), “ppar_signaling_pathway” (KEGG: hsa03320), “fatty_acid_metabolism” (KEGG: hsa00071), and “propanoate_metabolism” (KEGG: hsa00640) were also found to be enriched in livers from 24 h fasted PPARα+/+ relative to PPAR-/- mice, while “peroxisome” (KEGG: hsa04146),

436 "ppar_signaling_pathway" (KEGG: hsa03320), and "fatty_acid_metabolism" (KEGG:
437 hsa00071), were found to be enriched in livers from wild type mice treated with the PPARα
438 agonist Wy14643, relative to vehicle (Kersten 2014). Together, these studies support a
439 convergence of 10(*Z*)-hexadecenoic acid effects on PPARα signaling pathways induced by
440 physiological or pharmacological stimuli. Propionate is one of the short-chain fatty acids, which
441 are emerging as key mediators and regulators of host-microbe cross-talk, with a significant
442 impact on host metabolism, including as an energy source (Hoyles et al. 2018). All 5 gene sets
443 were significant with an unadjusted p value < 0.05, but failed to reach significance using FDR-
444 adjusted p values; nevertheless, the overall pattern is consistent with a modulation of lipid
445 metabolism. In a network visualization of gene set overlap between all detected pathways using
446 DAVID, PPARs and peroxisomal lipid metabolism were prominent vertices (Fig. 3D). We also
447 searched against the collection of transcription factor binding motifs (c3.tft.v6.0), which revealed
448 enrichment for CREB, Gfi1, and PPARα *cis*-regulatory motifs upstream of the genes upregulated
449 with 10(*Z*)-hexadecenoic acid treatment in LPS-stimulated macrophages (Table S7). Again, these
450 were nominally significant (i.e. $p < 0.05$; $q > 0.05$), but these findings bolster PPARs, and
451 specifically PPARα, as a potential receptor mediating anti-inflammatory effects of 10(*Z*)-
452 hexadecenoic acid.

453 ***Downstream signaling of TLR4 is inhibited with 10(Z)-hexadecenoic acid treatment***

454 NF-κB is one of three major transcription factors downstream of LPS-induced activation of toll-
455 like receptor 4 (TLR4), the other two being IRF3 and AP-1 (Kawasaki and Kawai 2014). Using
456 all expression data in GSEA, we found that pretreatment with 10(*Z*)-hexadecenoic acid, relative
457 to treatment with vehicle, prior to LPS stimulation, downregulated signaling pathways
458 downstream from TLR4, such as NF-κB and IRF3, but not AP-1. In a network visualization of

the most significant pathways (FDR < 0.1), there is a bifurcation at the "ZHOU_INFLAMMATORY_RESPONSE_LPS" node representing the NF-κB and IRF3 responses (Fig. 4A). Among all nodes in this network, we counted and ranked the occurrence of enriched transcripts. The counts for the highest ranking transcripts were categorized into either NF-κB regulated responses or IRF regulated responses (Fig. 4B). We also examined enrichment for transcription factor motifs and detected enrichment for NF-κB, IRF1, IRF2, and IRF_Q6 among others, in transcripts associated with the vehicle treated, LPS stimulated group (Table S8). Alternatively, this can be understood to mean that mRNA transcripts that are located near those transcription factor binding sites are downregulated in 10(*Z*)-hexadecenoic acid treated, LPS-stimulated macrophages. To better understand the classification of the IRF_Q6 gene set (N = 242 genes) and differentially expressed genes ($q < 0.1$, N = 203 genes), they were both queried against the Interferome database (Rusinova et al. 2013). There are three types of interferons (IFNs), namely type I (composed of α, β, κ, ε, and ω subtypes), type II (IFNγ) and type III (IFNλ; also called IL28 and IL29), which are distinguished by having distinct genetic loci, amino acid sequence homology and specific cognate receptors (Pestka et al. 2004). This analysis revealed that a vast majority of the differentially expressed genes are regulated by both type I and II interferon responses (Fig. 4C), consistent with the hypothesis that 10(*Z*)-hexadecenoic acid alters TLR4, IRF3, and interferon signaling. Of note, cells infected with *Mycobacterium tuberculosis* induce type I interferons, including IFNα and IFNβ, which are thought to promote infection with *M. tuberculosis* (Travar et al. 2016). Using enrichment tools, like GSEA and DAVID, these RNA-seq data suggest that both NF-κB and IRF3 pathways are downregulated in LPS-stimulated macrophages when treated with 10(*Z*)-hexadecenoic acid.

The anti-inflammatory effects of 10(*Z*)-hexadecenoic acid are mediated through PPARα

10(Z)-hexadecenoic acid specifically activates PPARα

Fatty acids can modulate inflammation via the activation of nuclear hormone receptors (Chinetti et al. 2000; Kidani and Bensinger 2012). Therefore, we assessed the nuclear receptor activation capacity of: 1) the triacylglycerol (TAG), 1,2,3-tri[*Z*-10-hexadecenoyl]glycerol; 2) the monoacylglycerol (MAG), 1-[*Z*-10-hexadecenoyl]glycerol; and 3) the free fatty acid (FFA), 10(*Z*)-hexadecenoic acid. We conducted reporter gene assays via the transfection of COS1 cells using GAL4-fusion ligand binding domains (LBDs) of various lipid-activated nuclear receptors (PPARα-LBD, PPARγ-LBD, PPARδ-LBD and RARα-LBD) along with a plasmid carrying MH100-TK-luciferase reporter (Chen and Evans 1995). Transfected cells were incubated with TAG, MAG, or FFA for 18 h and relative luciferase activity, normalized to β-galactosidase activity, was measured. Each reporter transfection was validated with the respective receptor agonist (PPARα, WY-14643; PPARγ, rosiglitazone (RSG); PPARδ, GW1516; RARα, AM580). Both the MAG and FFA, at concentrations of 80 μM, reliably increased PPARα-, but not PPARγ-, PPARδ, or RARα-regulated reporter expression (Fig. 5A-D). The triglyceride had no effect (Fig. 5A-D). Together, these results demonstrate that 10(*Z*)-hexadecenoic acid and its monoacylglycerol form selectively activate the PPARα receptor.

PPARα is required for anti-inflammatory effects of 10(Z)-hexadecenoic acid

Next, we investigated if this interaction was necessary for inhibiting LPS-stimulated release of IL-6. Agonists and antagonists of each PPAR were used to test if PPARα has a singular role in this process. The agonists and antagonists and their receptor specificities are listed in Table S9 Macrophages were incubated with a single PPAR antagonist for 1 h prior to treatment with either 200 μM 10(*Z*)-hexadecenoic acid or a PPAR agonist complementary to its respective PPAR antagonist. After another 1 h incubation period, the cells were stimulated with LPS (1 μg/ml),

and IL-6 was measured 12 h later. Only with the PPARα antagonist, GW 6471, could the anti-inflammatory effects of 10(*Z*)-hexadecenoic acid be significantly reversed (Fig. 6A). The effects of the PPARγ and –δ antagonists were comparable to media (Fig. 6A). These results suggest a selective interaction between 10(*Z*)-hexadecenoic acid and PPARα, as the PPARα antagonist, GW 6471, had no effect on macrophage viability (Fig. S4), while it was effective in reversing the anti-inflammatory effects of the PPARα agonist, WY-14643, as measured by IL-6 secretion in LPS-stimulated macrophages (Fig. S5). To further explore the role of PPARα in the anti-inflammatory effects of 10(*Z*)-hexadecenoic acid, we repeated the assay with freshly isolated peritoneal macrophages from adult male C57BL/6J wild type and PPARα$^{-/-}$ mice. As expected, 10(*Z*)-hexadecenoic acid suppressed LPS-stimulated IL-6 in macrophages from wild type C57BL/6J mice, but this effect was absent in macrophages from PPARα KO mice (Fig. 6B). This indicated a full reversal of the anti-inflammatory effect of 10(*Z*)-hexadecenoic acid and the necessity of PPARα in mediating the effect.

DISCUSSION

Here we characterized the monounsaturated C16 free fatty acid, 10(*Z*)-hexadecenoic acid, derived from *M. vaccae* NCTC 11659, a saprophytic bacterium with anti-inflammatory and immunoregulatory properties that previously has been shown to prevent stress-induced exaggeration of peripheral inflammation and neuroinflammation, and to prevent stress-induced exaggeration of anxiety- and fear-related defensive behavioral responses. In addition, we showed that 10(*Z*)-hexadecenoic acid induced a broad transcriptional repression of inflammatory gene markers (see, for example, Table S10-11) and suppressed IL-6 secretion from freshly isolated, LPS-stimulated, murine peritoneal macrophages. Furthermore, we showed that both the monoacylated glycerol, 1-[*Z*-10-hexadecenoyl]glycerol and 10(*Z*)-hexadecenoic acid activated

PPARα signaling, as measured by transfection assays. Finally, we showed that PPARα antagonists prevented the anti-inflammatory effects of 10(*Z*)-hexadecenoic acid in macrophages, while the *ex vivo* effects of the lipid were absent in macrophages isolated from PPARα-deficient mice.

Here we focused on effects of 10(*Z*)-hexadecenoic acid on peritoneal macrophages. Based on a number of lines of evidence, effects of 10(*Z*)-hexadecenoic acid actions on peritoneal macrophages may have important implications for CNS immunity and subsequent behavioral outcomes. Intraperitoneal administration of lipopolysaccharide is known to induce priming of hippocampal microglia and worsen CNS outcomes (Cunningham 2005, 2013; Cunningham et al. 2009). Although the mechanisms through which peripheral inflammation signals to the CNS to induce microglial priming and neuroinflammatory responses are not entirely clear, a number of potential signaling mechanisms have been proposed. These include: 1) entry of cytokines into the brain at circumventricular organs that have a reduced blood-brain barrier; 2) binding of cytokines to cerebral vascular endothelium, inducing the secretion of central neuroinflammatory mediators; 3) carrier-mediated transport of immune signals into the brain, across the blood-brain barrier; 4) migration of proinflammatory monocytes from the periphery to the CNS; and 5) activation of peripheral afferent nerves, including vagal and non-vagal pathways (Watkins et al. 1995; Maier et al. 1998; Maier 2003; Miller et al. 2010; Miller and Raison 2016).

Together, these data support the hypothesis that bacterially-derived 10(*Z*)-hexadecenoic acid may induce a form of macrophage “inflammation anergy” (i.e., a condition characterized by an absence of the normal immune response to a particular antigen, see, for example, (Smythies et al. 2005, 2010) through actions on PPARα. Peroxisome proliferator-activated receptors, PPARα, PPARγ, and PPARδ are ligand-activated nuclear receptors, each of which acts as a heterodimer

551 with retinoid X receptor (RXR), with potent anti-inflammatory properties, through interference
552 with proinflammatory transcription factor pathways (Chinetti et al. 2003). PPARα$^{-/-}$ mice have
553 increased vulnerability to chemically-induced colitis, experimental autoimmune encephalitis
554 (EAE, a model of multiple sclerosis) and experimentally-induced allergic asthma, consistent with
555 the hypothesis that endogenous PPARα suppresses inflammatory signaling in these models (for
556 review, (Bensinger and Tontonoz 2008)). Activation of PPARα in macrophages inhibits the
557 production of proinflammatory response markers, including IL-6, IL-1β, TNF, and inducible
558 nitric oxide synthase (Xu et al. 2005; Paukkeri et al. 2007). Interaction between PPARα and
559 TLR4 signaling has been observed in other endogenous systems, like vascular smooth muscle
560 cells, where responses to activation of TLR4 with LPS are mitigated by a PPARα agonist (Ji et
561 al. 2010). The anti-inflammatory effects were mediated, in part, by a reduction of tissue inhibitor
562 of metalloprotease-1 (TIMP-1), which was also reduced in our study (Table S3). PPARα-
563 mediated inhibition of TLR4 signaling has also been shown in enteric glial cells (Esposito et al.
564 2014), and a potential downstream target of PPARα-mediated suppression, TRIF, is required for
565 LPS-induced activation of microglia (Burfeind et al. 2018). TRIF KO mice have attenuated
566 expression of *Il6*, *Ccl2*, and *Cxcl2*, which were all also suppressed in our study (Table S3), in the
567 hypothalamus after peripheral LPS stimulation (Burfeind et al. 2018). Furthermore, bacterially-
568 derived agonists of PPARs have potential for modulation of host-acquired immunity; PPARs
569 have been found to regulate T cell survival, activation, and CD4^{+} T helper cell differentiation
570 into the Th1, Th2, Th17, and Treg lineages (Choi and Bothwell 2012).

571 Synthesis of 10(*Z*)-hexadecenoic acid by mycobacteria may be an example of molecular mimicry
572 of eukaryotic signaling. Endogenous host-derived agonists of PPARα include 16:1 isoforms of
573 palmitoleic acid (Kliewer et al. 1997; Kota et al. 2005), a lipokine released from adipose cells.

Palmitoleic acid localizes predominantly to nuclear fractions, consistent with a nuclear mechanism of action in host cells (Foryst-Ludwig et al. 2015), and is potently anti-inflammatory (Chan et al. 2015). In addition, the endocannabinoid, palmitoylethanolamide (PEA), acts as an agonist at PPARα (Verme et al. 2005; Guida et al. 2017). Of interest to trauma- and stressor-related psychiatric disorders, PEA induces potent antidepressant-like behavioral responses (Yu et al. 2011) and, through induction of cannabinoid 2 receptors, alters the phenotype of macrophages and microglia (Guida et al. 2017). Recent studies have demonstrated PEA increases biosynthesis of allopregnanolone, an endocannabinoid, in the spinal cord, brainstem, hippocampus and amygdala, effects that are associated with faster fear extinction learning and improvement of aggression in socially-isolated mice (Sasso et al. 2012; Locci and Pinna 2017; Pinna 2018). Future studies should determine if 10(*Z*)-hexadecenoic acid is sufficient to induce the enhanced fear extinction learning previously demonstrated using whole, heat-killed *M. vaccae* (Fox et al. 2017), and to what extent these effects are mediated by PPARα.

Mycobacteria are unique in that they accumulate triacylglycerols as intracellular lipophilic inclusions. For example, *M. smegmatis* accumulates triacylglycerols and the acyl chain composition varies depending on the growth medium (Garton et al. 2002). Monounsaturated fatty acids, $C_{16:1}$ hexadecenoic acid and $C_{18:1}$ octadecenoic acid were found to be high when bacteria were grown in nutrient rich Middlebrook 7H9 broth, relative to low-nitrogen Youmans' broth, but highest when bacteria were grown in Youmans' broth with monounsaturated oleic acid ((9*Z*)-octadec-9-enoic acid) supplementation. Thus, it is possible that mycobacteria synthesize and store triacylglycerols using environmental fatty acids as substrates, potentially for export to the cell envelope and release. If so, it may be possible to modify the immunoregulatory and anti-inflammatory potential of mycobacteria through modification of growth conditions.

Of potential importance, conjugated linoleic acids are bacterial metabolites. For example, specific members of the genus *Lactobacillus*, including *Lactobacillus reuteri*, and *L. plantarum*, as well as bifidobacteria, mediate the conversion of dietary linoleic acid into immunomodulatory conjugated linoleic acids (Coakley et al. 2003; Lee et al. 2003; Ogawa et al. 2005; Kishino et al. 2013). Most of the conjugated linoleic acid produced is located in the extracellular space (~98%) (Lee et al. 2003; Roman-Nunez et al. 2007), suggesting that bacterially-derived conjugated linoleic acids may be metabolic signaling molecules that modulate the host immune response. These bacterially-derived fatty acid metabolites include 10-hydroxy-*cis*-12-octadecenoic acid (HYA), *cis*-9,*trans*-11-linoleic acid, *trans*-9,*cis*-11-linoleic acid, and *cis*-10,*trans*-12-linoleic acid (Lee et al. 2003; Miyamoto et al. 2015), among many others (Ogawa et al. 2005). Several of these bacterially-derived fatty acid metabolites are potent PPARα agonists (IC_{50} values from 140 nM to 400 nM) (Moya-Camarena et al. 1999). Perhaps the closest analogue of 10(*Z*)-hexadecenoic acid identified here is trans-10-octadecenoic acid, produced by *L. plantarum* from linoleic acid (Kishino et al. 2013) or γ-linolenic acid (Ogawa et al. 2005). Although, to the best of our knowledge, the efficacy of trans-10-octadecenoic acid at PPARα receptors is not known, production of 10(*Z*)-hexadecenoic acid and diverse conjugated linoleic acids, which then act at host PPARα receptors, may be a general strategy of commensal organisms to suppress host immune responses, and promote symbiotic relationships with the host. Consistent with this hypothesis, macrophages lining the gut mucosa are anergic, characterized by an inability to mount proinflammatory responses, despite avid phagocytic activity (Smythies et al. 2005), while lung airway macrophages are immunoregulatory (Strickland et al. 1996; Soroosh et al. 2013; Duan and Croft 2014). Recent studies have also identified α-linolenic acid-derived bacterial metabolites, 13-hydroxy-9(*Z*),15(*Z*)-octadecadienoic acid (13-OH) and13-oxo-9(*Z*),15(*Z*)-

octadecadienoic acid (13-oxo), that induce differentiation of anti-inflammatory M2 macrophages through activation of G protein-coupled receptor 40 (GPR40) (Ohue-Kitano et al. 2018). Together, these data support the hypothesis that bacterially-derived "postbiotic" compounds, including fatty acid metabolites, have important beneficial effects on the host via diverse host receptor signaling mechanisms.

Although we did not assess the effects of 10(*Z*)-hexadecenoic acid on DCs or immunoregulation, defined as the balance between regulatory and effector T cells, conjugated linoleic acid suppresses NF-κB signaling and IL-12 production in DCs through IL-10 production (Loscher et al. 2005). Exposure of murine DCs to conjugated linoleic acid suppresses their ability to promote differentiation of naïve T cells into Th1 and/or Th17 cells *in vitro* following their adoptive transfer *in vivo* (Draper et al. 2014). Future studies should investigate the effects of 10(*Z*)-hexadecenoic acid on inflammatory signaling in macrophages, DCs, as well as on T cell differentiation and function, the potential role of PPARα in these effects, and consequences for stress-induced exaggeration of anxiety- and fear-related behavioral responses.

Overall, our data suggest that chemical mimicry of eukaryotic signaling molecules may be common among environmental bacteria, including mycobacteria (Gebert et al. 2018), that are abundant in host mucosal surfaces (Macovei et al. 2015), and bacterially-derived anti-inflammatory lipids have potential as a novel approach to therapeutic intervention in inflammatory disease and stress-related psychiatric disorders, where immunodysregulation and inappropriate inflammation have been identified as risk factors (Rohleder 2014; Langgartner et al. 2018).

AUTHOR CONTRIBUTIONS

642 G.S.B and P.A.I. isolated and synthesized 1,2,3-tri[*Z*-10-hexadecenoyl]glycerol. W.X. and X.W.
643 developed a synthesis for 10(*Z*)-hexadecenoic acid and synthesized the compound. Experimental
644 design was done by D.G.S., R.M., G.S.B., G.A.W.R., L.R.B., and C.A.L. L.N. and P.A.I
645 designed the PPAR experiments. *In vivo* screening and experimentation was performed by R.M.,
646 and L.R.B. *In vitro* experiments using freshly isolated murine peritoneal macrophages were
647 performed by D.G.S. Transfections and reporter gene assays were performed by I.S. and P.B.
648 RNA-seq data processing and analysis was done by D.G.S., R.D.D., M.A.A. Experimental
649 design and preparation of the manuscript were done by D.G.S., R.M., G.S.B., L.N., G.A.W.R.,
650 L.R.B., and C.A.L.

651

FIGURE LEGENDS

Fig. 1 Experimental timeline for *ex vivo* macrophage stimulation.

Abbreviations: FFA; free fatty acid, LPS, lipopolysaccharide.

Fig. 2 Anti-inflammatory effects of 10(*Z*)-hexadecenoic acid in freshly-isolated murine peritoneal macrophages.

Freshly isolated murine peritoneal macrophages were incubated for 1 h with synthetic 10(*Z*)-hexadecenoic acid (0.4 μM, 4 μM, 20 μM, 100 μM, 500 μM, 1000 μM), then challenged with lipopolysaccharide (LPS; 1 μg/mL). Cell supernatants were collected at (**A**) 6 h, (**B**) 12 h, and (**C**) 24 h after lipopolysaccharide (LPS) challenge. Interleukin (IL) 6 concentrations in the supernatant were determined using enzyme-linked immunosorbent assay (ELISA) and reported relative to media-only controls (n = 6 replicates, with each replicate using different freshly isolated peritoneal macrophages; each sample was run using duplicate wells in the ELISA). Data were fit with a logistic function, which was used to estimate the EC50. Data are expressed as mean ± SEM.

Fig. 3 Gene networks upregulated following pretreatment with 10(*Z*)-hexadecenoic acid in LPS-stimulated macrophages suggest anti-inflammatory effects are mediated by PPARα.

Murine peritoneal macrophages were treated with either 10(*Z*)-hexadecenoic acid (200 μM) or vehicle. Following a 12 h period after stimulation with lipopolysaccharide (LPS), total RNA content was measured using RNA-seq. (**A**) Heat map of the top 20 differentially expressed transcripts. (**B**) and (**C**) Genes significantly (**B**) upregulated or (**C**) downregulated with treatment of 10(*Z*)-hexadecenoic acid were separately queried on the Database for Annotation, Visualization and Integrated Discovery (DAVID). (**B**) The top five Kyoto Encyclopedia of

Genes and Genomes (KEGG) pathways enriched for genes upregulated following pretreatment of LPS-stimulated macrophages with 10(*Z*)-hexadecenoic acid, relative to media pretreated, LPS-stimulated macrophages. (**C**) The top five KEGG pathways enriched for genes downregulated following pretreatment of LPS-stimulated macrophages with 10(*Z*)-hexadecenoic acid, relative to media pretreated, LPS-stimulated macrophages. (**D**) Pathway analysis using the entire transcriptional data set was performed with Gene Set Enrichment Analysis (GSEA). Pathways enriched for genes upregulated following pretreatment of LPS-stimulated macrophages with 10(*Z*)-hexadecenoic acid, relative to media-pretreated, LPS-stimulated macrophages, were visualized in a network built by their gene set overlap. The size of the network node represents the number of genes shared between the particular gene set and the transcription data. The weight of network edges represents the degree of gene set overlap. In the largest cluster of pathways enriched in genes upregulated with 10(*Z*)-hexadecenoic acid, lipid metabolism and peroxisome proliferator-activated receptors (PPARs) were implicated as some of the more salient pathways. Abbreviations: Adamtsl4, thrombospondin repeat-containing protein 1; AMPK, 5' AMP-activated protein kinase; Ch25h, cholesterol 25-hydroxylase; Cish, cytokine inducible SH2 containing protein; Ctla2b, cytotoxic T-lymphocyte-associated protein 2-beta; Cyp26b1, cytochrome P450 family 26 subfamily B member 1; Dusp1, dual specificity phosphatase 1; ECM, extracellular matrix; F3, coagulation factor III; Flrt3, fibronectin leucine rich transmembrane protein 3; Hdc, histidine decarboxylase; Hp, haptoglobin; Il1b, interleukin 1 beta; Il6, interleukin 6; LKB1, liver kinase B1; Mir5105, microRNA 5105; MTOR, mechanistic target of rapamycin kinase; Plbd1, phospholipase B domain containing 1; Plin2, perilipin 2; PPAR, peroxisome proliferator activated receptor; PPARA, peroxisome proliferator activated receptor alpha; Ptgs2, prostaglandin-endoperoxide synthase 2; RORA, RAR related orphan

receptor A; TNF, tumor necrosis factor; Tns1, tensin 1; Tsc22d3, Tsc22 domain family member 3; Vnn3, vanin 3.

Fig. 4. 10(*Z*)-hexadecenoic acid suppresses expression of transcription factors downstream of TLR4.
Murine peritoneal macrophages were treated with either 10(*Z*)-hexadecenoic acid (200 μM) or vehicle for 1 h, then challenged with lipopolysaccharide (LPS; 1 μg/ml). Following a 12 h period after stimulation with LPS, mRNA was measured using RNA-seq. (**A**) From Gene Set Enrichment Analysis (GSEA; c2.all.v6.2), pathways enriched with genes downregulated following pretreatment of LPS-stimulated macrophages with 10(*Z*)-hexadecenoic acid, relative to media-pretreated, LPS-stimulated macrophages, were visualized in a network built by their gene set overlap. The size of the network node indicates the number of genes shared between the particular gene set and the transcription data from our study. The weight of network edges indicates the degree of gene set overlap between nodes. The color of the node indicates whether the genes in the gene set are upregulated in NF-κB pathways (blue), upregulated in IRF pathways (purple), ambiguously upregulated (gray), or downregulated (red). (**B**) Among the leading edges of enriched pathway gene sets, the occurrence of high ranking genes in either the NF-κB-regulated network (blue) or IRF-regulated network (purple) (corresponding to data illustrated in panel A) are reported. (**C**) Genes included in the IRF_Q6 gene set (left; i.e., genes having at least one occurrence of the transcription factor binding site V$IRF_Q6 (v7.4 TRANSFAC) in the regions spanning up to 4 kb around their transcription starting sites) and the significant 10(*Z*)-hexadecenoic acid-dependent differentially expressed genes with $q < 0.1$ (right) were queried against the Interferome database (v2.0) to identify their association with known interferon responses. The majority of genes in both gene sets are attributed to both Type I and Type II

721 interferon responses. Abbreviations: CCL2, C-C motif chemokine ligand 2; CXCL1, C-X-C
722 motif chemokine ligand 1; CXCL2, C-X-C motif chemokine ligand 2; IER3, immediate early
723 response 3; IFN, interferon; IFNA, interferon alpha; IFNB1, interferon beta 1; IKK, inhibitor of
724 nuclear factor kappa B kinase; INHBA, inhibin subunit beta A; IL1A, interleukin 1 alpha; IL1B,
725 interleukin 1 beta; IL1R, interleukin 1 receptor; IL6, interleukin 6; JUNB, junB proto-oncogene,
726 AP-1 transcription factor subunit; LPS, lipopolysaccharide; NFKB, nuclear factor kappa B;
727 NFKB1, nuclear factor kappa B subunit 1; PLAUR, plasminogen activator, urokinase receptor;
728 PSMB8, proteasome subunit beta 8; PSMB9, proteasome subunit beta 9; PSMB10, proteasome
729 subunit beta 10; PSME1, proteasome activator subunit 1; PTGS2, prostaglandin-endoperoxide
730 synthase 2; STAT3, signal transducer and activator of transcription 3; TNF, tumor necrosis
731 factor.

732

733 **Fig. 5 Analysis of the effects of *M. vaccae*-derived lipids on peroxisome proliferator-**
734 **activated receptor (PPAR) α, PPARγ, PPARδ, and retinoic acid receptor (RAR) α signaling**
735 **in transfection assays using COS-1 cells.**

736 (**A**) Relative activity of PPARα following incubation with the 1,2,3-tri[*Z*-10-
737 hexadecenoyl]glycerol (PI-70; TAG), monoacylglycerol, 1-[*Z*-10-hexadecenoyl]glycerol (PI-69;
738 MAG), or 10(*Z*)-hexadecenoic acid (PI-71; FFA) for 18 h, expressed as relative luciferase
739 activity, normalized to β-galactosidase activity. (**B**) Relative activity of PPARγ. (**C**) Relative
740 activity of PPARδ. (**D**) Relative activity of RARα. Abbreviations and concentrations: AM580
741 (RARα-specific agonist, 100 nM), GW1516 (PPARδ agonist, 1 μM), RSG, rosiglitazone
742 (PPARγ agonist, 2.5 μM), troglitazone (PPARγ agonist, 10 μM), WY-14643 (PPARα agonist, 2
743 μM). Data are representative of 2-3 replicates per experiment.

Fig. 6 PPARα is required for suppression of LPS-induced inflammation in macrophages.

A peroxisome proliferator-activated receptor (PPAR) α, -γ, or -δ antagonist (GW 6471, GW 9662, GSK 0660 respectively) or vehicle was applied to murine peritoneal macrophages followed by treatment with either 10(*Z*)-hexadecenoic acid (200 μM), vehicle, or dexamethasone (Dex; 10 μM), then stimulated with lipopolysaccharide (LPS; 1 μg/ml). (**A**) After 12 h, interleukin (IL) 6 was measured in the cell supernatant and reported relative to vehicle controls. (**B**) The necessity of PPARα was shown in a PPARα knock out (KO) model. Murine peritoneal macrophages from PPARα$^{-/-}$ or WT mice were incubated with either 10(*Z*)-hexadecenoic acid (50 μM or 200 μM) or vehicle, then stimulated with LPS (1 μg/ml). #$p < 0.05$, Fisher's least significant difference (LSD), relative to cells only treated with 10(*Z*)-hexadecenoic acid. *$p < 0.05$ relative to KO.

SUPPORTING INFORMATION TITLES AND CAPTIONS

Table S1. Dose- and time-dependent effects of 10(Z)-hexadecenoic acid on secretion of IL-6 from freshly isolated murine peritoneal macrophages stimulated with lipopolysaccharide.

Table S2. Descriptive statistics of cDNA libraries and RNA-sequencing.

Table S3. List of 203 differentially expressed genes between treatment with 10(*Z*)-hexadecenoic acid and vehicle in LPS-stimulated macrophages (FDR-adjusted $p < 0.1$)

Table S4. KEGG pathways and GO biological processes with associated genes that are significantly downregulated in LPS-stimulated murine macrophages preincubated with 10(*Z*)-hexadecenoic acid, relative to LPS-stimulated murine macrophages preincubated with media.

765 **Table S5. Top scoring KEGG pathways enriched for differentially expressed genes (*q* <**
766 **0.1).**

767 **Table S6. Top scoring KEGG pathway enrichment scores of 10(*Z*)-hexadecenoic acid**
768 **treatment**

769 **Table S7. Transcription factor binding site enrichment scores of 10(*Z*)-hexadecenoic acid**
770 **treatment**

771 **Table S8. Transcription factor binding site enrichment scores of DMEM (i.e., LPS**
772 **exposure, in the absence of 10(*Z*)-hexadecenoic acid treatment)**

773 **Table S9. Selective peroxisome proliferator-activated receptor (PPAR) antagonists and**
774 **agonists.**

775 **Table S10**. **Lipopolysaccharide-induced proinflammatory cytokine and chemokine ligand**
776 **mRNAs downregulated by preincubation of freshly isolated murine peritoneal**
777 **macrophages with 10(*Z*)-hexadecenoic acid (selected from 203 differentially expressed**
778 **mRNAs)**

779 **Fig. S1. 10(*Z*)-hexadecenoic acid alone has no detectable effect on IL-6 release.**

780 After isolation of peritoneal macrophages and incubation with 10(*Z*)-hexadecenoic acid for 1 h,
781 macrophages were challenged with either lipopolysaccharide (LPS) or Dulbecco's Modified
782 Eagle Medium (DMEM; as control). There was no detectable effect of 10(*Z*)-hexadecenoic acid
783 on interleukin (IL) 6 secretion in the cultures that did not receive LPS. Abbreviations: IL-6,
784 interleukin 6; LPS, lipopolysaccharide. Data are representative of 3 replicates per condition.

785 **Fig. S2. Effect of 10(*Z*)-hexadecencoic acid on macrophage cell viability.**

Sulforhodamine B (SRB) was used to assess cytotoxic effects of various concentrations of synthetic 10(*Z*)-hexadecenoic acid (10 µM, 50 µM, 125 µM, 250 µM, 500 µM, 1000 µM) after 0, 6, 12, 24, 48, and 72 h of incubation with freshly isolated murine peritoneal macrophages. Percent control growth is expressed as % viability and is a ratio of the amount of growth that occurred with treatment over the amount of growth that occurred in media. One hundred percent indicates no differences in cell growth between treatment and media, whereas values below 100% indicate that growth was impaired with treatment. Data are expressed as mean ± SEM of 3-7 mice per condition.

Fig. S3. BioAnalyzer electropherograms of cDNA libraries used for RNA-sequencing. Total RNA content of $1x10^5$ macrophages was prepared for each sample utilizing separate macrophage preparations from $n = 3$ mice treated with vehicle (Dulbecco's Modified Eagle Medium (DMEM; upper row) then challenged with 1µg/mL lipopolysaccharide (LPS) or $n = 3$ mice treated with 200 µM 10(*Z*)-hexadecenoic acid for 1 h, then challenged with 1µg/mL LPS. Macrophages were harvested 12 h following LPS challenge. Peaks at 35 bp and 10,380 bp are gel migration markers.

Fig. S4. Effect of PPAR agonists and antagonists on macrophage cell viability.

Sulforhodamine B (SRB) was used to assess cytotoxic effects of PPAR agonists (PPARα, WY-14643; PPARγ, rosiglitazone (RSG); PPARδ, GW0742) or PPAR agonists and antagonists (PPARα, GW6471; PPARγ, GW9662; PPARδ, GSK0660). The agonists and antagonists were incubated with freshly isolated murine peritoneal macrophages at 2x their respective EC50 or IC50 (see Table S9). Percent control growth is expressed as % viability and is a ratio of the

amount of growth that occurred with treatment over the amount of growth that occurred in media. One hundred percent indicates no differences in cell growth between treatment and media, whereas values below 100% indicate that growth was impaired with treatment. Data are expressed as mean ± SEM of 3-7 mice per condition.

Figure S5. Suppression of IL-6 in LPS-stimulated macrophages is achieved through activation of PPARα and reversed by addition of a PPARα antagonist.

Murine peritoneal macrophages were incubated with peroxisome proliferator-activated receptor (PPAR) α antagonist (GW 6471), PPARγ antagonist (GW 9662), PPARδ antagonist (GSK 0660), or Dulbecco's Modified Eagle Medium (DMEM)/F-12. After a 1-h incubation, the cells were treated with the complementary agonist (PPARα: WY-14643, PPARγ: rosiglitazone; Rosi., PPARδ: GW 0742). For each agonist, four concentrations were assayed, 1x, 2x, 5x, and 10x the half-maximal effective concentration (EC_{50}). The immune response was measured as the concentration of interleukin (IL) 6 in the cell supernatant relative to vehicle controls. #$p < 0.05$ main effect of agonist + antagonist condition relative to agonist alone condition in a multifactor ANOVA. *$p < 0.05$, Fisher's least significant difference (LSD), pairwise comparison relative to antagonist-treated cells.

827 **REFERENCES**

828 Adams VC, Hunt JRF, Martinelli R, et al (2004) *Mycobacterium vaccae* induces a population of
829 pulmonary CD11c+ cells with regulatory potential in allergic mice. Eur J Immunol 34:631–
830 638. doi: 10.1002/eji.200324659

831 American Psychiatric Association (2013) Diagnostic and Statistical Manual DSM 5

832 Anders S, Huber W (2010) Differential expression analysis for sequence count data. Genome
833 Biol 11:R106. doi: 10.1186/gb-2010-11-10-r106

834 Anders S, Pyl PT, Huber W (2015) HTSeq-A Python framework to work with high-throughput
835 sequencing data. Bioinformatics 31:166–169. doi: 10.1093/bioinformatics/btu638

836 Arteaga Figueroa L, Abarca-Vargas R, García Alanis C, Petricevich VL (2017) Comparison
837 between Peritoneal Macrophage Activation by *Bougainvillea xbuttiana* Extract and LPS
838 and/or Interleukins. Biomed Res Int. doi: 10.1155/2017/4602952

839 Baxter AJ, Scott KM, Vos T, Whiteford HA (2013) Global prevalence of anxiety disorders: A
840 systematic review and meta-regression. Psychol. Med.

841 Benko S, Love JD, Beládi M, et al (2003) Molecular determinants of the balance between co-
842 repressor and co-activator recruitment to the retinoic acid receptor. J Biol Chem
843 278:43797–43806. doi: 10.1074/jbc.M306199200

844 Bensinger SJ, Tontonoz P (2008) Integration of metabolism and inflammation by lipid-activated
845 nuclear receptors. Nature 454:470–7. doi: 10.1038/nature07202

846 Blaser MJ (2017) The theory of disappearing microbiota and the epidemics of chronic diseases.
847 Nat. Rev. Immunol. 17:461–463

848 Bloomfield SF, Rook GA, Scott EA, et al (2016) Time to abandon the hygiene hypothesis: new
849 perspectives on allergic disease, the human microbiome, infectious disease prevention and
850 the role of targeted hygiene. Perspect Public Health 136:213–224. doi:
851 10.1177/1757913916650225

852 Bolger AM, Lohse M, Usadel B (2014) Trimmomatic: A flexible trimmer for Illumina sequence
853 data. Bioinformatics 30:2114–2120. doi: 10.1093/bioinformatics/btu170

854 Böttger EC, Hirschel B, Coyle MB (1993) *Mycobacterium genavense*. Int J Syst Bacteriol
855 43:841–843. doi: 10.1099/00207713-43-4-841

856 Burfeind KG, Zhu X, Levasseur PR, et al (2018) TRIF is a key inflammatory mediator of acute
857 sickness behavior and cancer cachexia. Brain Behav Immun 73:364–374. doi:
858 10.1016/j.bbi.2018.05.021

859 Chan KL, Pillon NJ, Sivaloganathan DM, et al (2015) Palmitoleate reverses high fat-induced
860 proinflammatory macrophage polarization via AMP-activated protein kinase (AMPK). J
861 Biol Chem 290:16979–16988. doi: 10.1074/jbc.M115.646992

862 Chen JD, Evans RM (1995) A transcriptional co-repressor that interacts with nuclear hormone
863 receptors. Nature 377:454–457

864 Chinetti G, Fruchart JC, Staels B (2000) Peroxisome proliferator-activated receptors (PPARs):
865 Nuclear receptors at the crossroads between lipid metabolism and inflammation. Inflamm.
866 Res. 49:497–505

867 Chinetti G, Fruchart JC, Staels B (2003) Peroxisome proliferator-activated receptors: new targets
868 for the pharmacological modulation of macrophage gene expression and function. Curr

869 Opin Lipidol 14:459–468. doi: 10.1097/01.mol.0000092630.86399.00

870 Choi JM, Bothwell ALM (2012) The nuclear receptor PPARs as important regulators of T-cell
871 functions and autoimmune diseases. Mol. Cells 33:217–222

872 Chou S, Chedore P, Kasatiya S (1998) Use of gas chromatographic fatty acid and mycolic acid
873 cleavage product determination to differentiate among *Mycobacterium genavense*,
874 *Mycobacterium fortuitum*, *Mycobacterium simiae*, and *Mycobacterium tuberculosis*. J Clin
875 Microbiol 36:577–579

876 Coakley M, Ross RP, Nordgren M, et al (2003) Conjugated linoleic acid biosynthesis by human-
877 derived *Bifidobacterium species*. J Appl Microbiol 94:138–145. doi: 10.1046/j.1365-
878 2672.2003.01814.x

879 Coyle MB, Carlson LDC, Wallis CK, et al (1992) Laboratory aspects of *Mycobacterium*
880 *genavense*, a proposed species isolated from AIDS patients. J Clin Microbiol

881 Cryan JF, Dinan TG (2015) More than a Gut Feeling: The Microbiota Regulates
882 Neurodevelopment and Behavior. Neuropsychopharmacology

883 Cryan JF, Dinan TG (2012) Mind-altering microorganisms: the impact of the gut microbiota on
884 brain and behaviour. Nat Rev Neurosci 13:701–12. doi: 10.1038/nrn3346

885 Cunningham C (2005) Central and Systemic Endotoxin Challenges Exacerbate the Local
886 Inflammatory Response and Increase Neuronal Death during Chronic Neurodegeneration. J
887 Neurosci. doi: 10.1523/jneurosci.2614-05.2005

888 Cunningham C (2013) Microglia and neurodegeneration: The role of systemic inflammation.
889 Glia. doi: 10.1002/glia.22350

890 Cunningham C, Campion S, Lunnon K, et al (2009) Systemic Inflammation Induces Acute
891 Behavioral and Cognitive Changes and Accelerates Neurodegenerative Disease. Biol
892 Psychiatry. doi: 10.1016/j.biopsych.2008.07.024

893 Draper E, DeCourcey J, Higgins SC, et al (2014) Conjugated linoleic acid suppresses dendritic
894 cell activation and subsequent Th17 responses. J Nutr Biochem 25:741–749. doi:
895 10.1016/j.jnutbio.2014.03.004

896 Duan W, Croft M (2014) Control of regulatory T Cells and airway tolerance by lung
897 macrophages and dendritic cells. Ann Am Thorac Soc 11:S306–S313. doi:
898 10.1513/AnnalsATS.201401-028AW

899 Esposito G, Capoccia E, Turco F, et al (2014) Palmitoylethanolamide improves colon
900 inflammation through an enteric glia/toll like receptor 4-dependent PPAR-α activation. Gut
901 63:1300–1312. doi: 10.1136/gutjnl-2013-305005

902 Forsythe P, Sudo N, Dinan T, et al (2010) Mood and gut feelings. Brain Behav Immun 24:9–16.
903 doi: 10.1016/j.bbi.2009.05.058

904 Foryst-Ludwig A, Kreissl MC, Benz V, et al (2015) Adipose tissue lipolysis promotes exercise-
905 induced cardiac hypertrophy involving the lipokine C16: 1n7-palmitoleate. J Biol Chem
906 290:23603–23615. doi: 10.1074/jbc.M115.645341

907 Fox JH, Hassell JE, Siebler PH, et al (2017) Preimmunization with a heat-killed preparation of
908 *Mycobacterium vaccae* enhances fear extinction in the fear-potentiated startle paradigm.
909 Brain Behav Immun. doi: 10.1016/j.bbi.2017.08.014

910 Frank MG, Fonken LK, Dolzani SD, et al (2018) Immunization with *Mycobacterium vaccae*

911 induces an anti-inflammatory milieu in the CNS: Attenuation of stress-induced microglial
912 priming, alarmins and anxiety-like behavior. Brain Behav Immun 73:352–363. doi:
913 10.1016/j.bbi.2018.05.020

914 Garn H, Bahn S, Baune BT, et al (2016) Current concepts in chronic inflammatory diseases:
915 Interactions between microbes, cellular metabolism, and inflammation. J Allergy Clin
916 Immunol 138:47–56. doi: 10.1016/j.jaci.2016.02.046

917 Garton NJ, Christensen H, Minnikin DE, et al (2002) Intracellular lipophilic inclusions of
918 mycobacteria *in vitro* and in sputum. Microbiology 148:2951–2958. doi:
919 10.1099/00221287-148-10-2951

920 Gebert MJ, Delgado-baquerizo M, Oliverio AM, et al (2018) Ecological analyses of
921 mycobacteria in showerhead biofilms and their relevance to human health. bioRxiv. doi:
922 10.1101/366088

923 Guida F, Luongo L, Boccella S, et al (2017) Palmitoylethanolamide induces microglia changes
924 associated with increased migration and phagocytic activity: Involvement of the CB2
925 receptor. Sci Rep 7:1–11. doi: 10.1038/s41598-017-00342-1

926 Gutzwiller MER, Reist M, Peel JE, et al (2007) Intradermal injection of heat-killed
927 *Mycobacterium vaccae* in dogs with atopic dermatitis: A multicentre pilot study. Vet
928 Dermatol 18:87–93. doi: 10.1111/j.1365-3164.2007.00579.x

929 Hoyles L, Snelling T, Umlai UK, et al (2018) Microbiome–host systems interactions: Protective
930 effects of propionate upon the blood–brain barrier. Microbiome. doi: 10.1186/s40168-018-
931 0439-y

932 Huang DW, Sherman BT, Lempicki RA, et al (2009) Bioinformatics enrichment tools: paths
933 toward the comprehensive functional analysis of large gene lists. Nucleic Acids Res 37:1–
934 13. doi: 10.1093/nar/gkn923

935 Ji Y, Wang Z, Li Z, Liu J (2010) Modulation of LPS-mediated inflammation by fenofibrate via
936 the TRIF-dependent TLR4 signaling pathway in vascular smooth muscle cells. Cell Physiol
937 Biochem 25:631–640. doi: 10.1159/000315082

938 Kawasaki T, Kawai T (2014) Toll-like receptor signaling pathways. Front. Immunol.

939 Kersten S (2014) Integrated physiology and systems biology of PPARα. Mol Metab 3:354–371.
940 doi: 10.1016/j.molmet.2014.02.002

941 Kidani Y, Bensinger S (2012) Liver X receptor and peroxisome proliferator-activated receptor as
942 integrators of lipid homeostasis and immunity. Immunol Rev 249:72–83. doi:
943 10.1111/j.1600-065X.2012.01153.x

944 Kilkenny C, Altman DG (2010) Improving bioscience research reporting: ARRIVE-ing at a
945 solution. Lab Anim. doi: 10.1258/la.2010.0010021

946 Kim D, Pertea G, Trapnell C, et al (2013) TopHat2: accurate alignment of transcriptomes in the
947 presence of insertions, deletions and gene fusions. Genome Biol 14:R36. doi: 10.1186/gb-
948 2013-14-4-r36

949 Kishino S, Takeuchi M, Park S-B, et al (2013) Polyunsaturated fatty acid saturation by gut lactic
950 acid bacteria affecting host lipid composition. Proc Natl Acad Sci U S A 110:. doi:
951 10.1073/pnas.1312937110

952 Kliewer SA, Sundseth SS, Jones SA, et al (1997) Fatty acids and eicosanoids regulate gene

953 expression through direct interactions with peroxisome proliferator-activated receptors
954 alpha and gamma. Proc Natl Acad Sci U S A 94:4318–23. doi: 10.1073/pnas.94.9.4318

955 Kota BP, Huang THW, Roufogalis BD (2005) An overview on biological mechanisms of
956 PPARs. Pharmacol. Res. 51:85–94

957 Langgartner D, Lowry CA, Reber SO (2018) Old Friends, immunoregulation, and stress
958 resilience. Pflügers Arch - Eur J Physiol. doi: 10.1007/s00424-018-2228-7

959 Le Bert N, Chain BM, Rook G, Noursadeghi M (2011) DC priming by M. vaccae inhibits Th2
960 responses in contrast to specific TLR2 priming and is associated with selective activation of
961 the CREB pathway. PLoS One 6:e18346. doi: 10.1371/journal.pone.0018346

962 Leclercq S, Forsythe P, Bienenstock J (2016) Posttraumatic Stress Disorder: Does the Gut
963 Microbiome Hold the Key? Can J Psychiatry. doi: 10.1177/0706743716635535

964 Lee AJ, Cho KJ, Kim JH (2015) MyD88-BLT2-dependent cascade contributes to LPS-induced
965 interleukin-6 production in mouse macrophage. Exp Mol Med. doi: 10.1038/emm.2015.8

966 Lee SO, Hong GW, Oh DK (2003) Bioconversion of linoleic acid into conjugated linoleic acid
967 by immobilized *Lactobacillus reuteri*. Biotechnol Prog 19:1081–4. doi: 10.1021/bp0257933

968 Lin JY, Tang CY (2007) Interleukin-10 administration inhibits TNF-alpha and IL-1beta, but not
969 IL-6, secretion of LPS-stimulated peritoneal macrophages. J Food Drug Anal

970 Locci A, Pinna G (2017) Neurosteroid biosynthesis down-regulation and changes in
971 GABAAreceptor subunit composition: a biomarker axis in stress-induced cognitive and
972 emotional impairment. Br. J. Pharmacol.

973 Loscher CE, Draper E, Leavy O, et al (2005) Conjugated linoleic acid suppresses NF-κB

974 activation and IL-12 production in dendritic cells through ERK-mediated IL-10 induction. J
975 Immunol 175:4990–4998. doi: 175/8/4990 [pii]

976 Lowry C a, Hollis JH, de Vries a, et al (2007) Identification of an immune-responsive
977 mesolimbocortical serotonergic system: potential role in regulation of emotional behavior.
978 Neuroscience 146:756–72. doi: 10.1016/j.neuroscience.2007.01.067

979 Lowry CA, Smith DG, Siebler PH, et al (2016) The microbiota, immunoregulation, and mental
980 health: implications for public health. Curr Environ Health Rep 3:270–286. doi:
981 10.1007/s40572-016-0100-5

982 Lyte M, Cryan JF (2014) Microbial Endocrinology: The Microbiota- Gut-Brain Axis in Health
983 and Disease

984 Macovei L, McCafferty J, Chen T, et al (2015) The hidden “mycobacteriome” of the human
985 healthy oral cavity and upper respiratory tract. J Oral Microbiol 7:1–11. doi:
986 10.3402/jom.v7.26094

987 Maier SF (2003) Bi-directional immune-brain communication: Implications for understanding
988 stress, pain, and cognition. Brain. Behav. Immun.

989 Maier SF, Goehler LE, Fleshner M, Watkins LR (1998) The role of the vagus nerve in cytokine-
990 to-brain communication. In: Annals of the New York Academy of Sciences

991 Merico D, Isserlin R, Bader GD (2011) Visualizing gene-set enrichment results using the
992 cytoscape plug-in enrichment map. Methods Mol Biol 781:257–277. doi: 10.1007/978-1-
993 61779-276-2_12

994 Miller AH, Maletic V, Raison CL (2010) Inflammation and its discontents: The role of cytokines

995 in the pathophysiology of major depression. Psiquiatr. Biol.

996 Miller AH, Raison CL (2016) The role of inflammation in depression: From evolutionary
997 imperative to modern treatment target. Nat. Rev. Immunol.

998 Miyamoto J, Mizukure T, Park SB, et al (2015) A gut microbial metabolite of linoleic acid, 10-
999 hydroxy-cis-12-octadecenoic acid, ameliorates intestinal epithelial barrier impairment
1000 partially via GPR40-MEK-ERK pathway. J Biol Chem 290:2902–2918. doi:
1001 10.1074/jbc.M114.610733

1002 Moya-Camarena SY, Vanden Heuvel JP, Blanchard SG, et al (1999) Conjugated linoleic acid is
1003 a potent naturally occurring ligand and activator of PPARα. J Lipid Res 40:1426–1433. doi:
1004 10.1631/jzus.B1200175

1005 Nagy L, Kao HY, Love JD, et al (1999) Mechanism of corepressor binding and release from
1006 nuclear hormone receptors. Genes Dev 13:3209–3216. doi: 10.1101/gad.13.24.3209

1007 Nugent NR, Tyrka AR, Carpenter LL, Price LH (2011) Gene-environment interactions: Early
1008 life stress and risk for depressive and anxiety disorders. Psychopharmacology (Berl).

1009 O'Donovan A, Cohen BE, Seal KH, et al (2015) Elevated risk for autoimmune disorders in iraq
1010 and afghanistan veterans with posttraumatic stress disorder. Biol Psychiatry. doi:
1011 10.1016/j.biopsych.2014.06.015

1012 Ogawa J, Kishino S, Ando A, et al (2005) Production of conjugated fatty acids by lactic acid
1013 bacteria. J Biosci Bioeng 100:355–64. doi: 10.1263/jbb.100.355

1014 Ohue-Kitano R, Yasuoka Y, Goto T, et al (2018) A-Linolenic acid–derived metabolites from gut
1015 lactic acid bacteria induce differentiation of anti-inflammatory M2 macrophages through G

protein-coupled receptor 40. FASEB J. doi: 10.1096/fj.201700273R

Okada H, Kuhn C, Feillet H, Bach J-F (2010) The “hygiene hypothesis” for autoimmune and allergic diseases: an update. Clin Exp Immunol 160:1–9. doi: 10.1111/j.1365-2249.2010.04139.x

Pacífico C, Fernandes P, de Carvalho CCCR (2018) Mycobacterial response to organic solvents and possible implications on cross-resistance with antimicrobial agents. Front Microbiol. doi: 10.3389/fmicb.2018.00961

Paukkeri EL, Leppänen T, Sareila O, et al (2007) PPARα agonists inhibit nitric oxide production by enhancing iNOS degradation in LPS-treated macrophages. Br J Pharmacol 152:1081–1091. doi: 10.1038/sj.bjp.0707477

Pestka S, Krause CD, Walter MR (2004) Interferons, interferon-like cytokines, and their receptors. Immunol. Rev.

Pinna G (2018) Biomarkers for PTSD at the Interface of the Endocannabinoid and Neurosteroid Axis. Front Neurosci 12:482. doi: 10.3389/fnins.2018.00482

Reber SO, Siebler PH, Donner NC, et al (2016) Immunization with a heat-killed preparation of the environmental bacterium *Mycobacterium vaccae* promotes stress resilience in mice. Proc Natl Acad Sci 113:3130–3139. doi: 10.1073/pnas.1600324113

Rohleder N (2014) Stimulation of systemic low-grade inflammation by psychosocial stress. Psychosom. Med.

Roman-Nunez M, Cuesta-Alonso EP, Gilliland SE (2007) Influence of sodium glycocholate on production of conjugated linoleic acid by cells of *Lactobacillus reuteri* ATCC 55739. J

1037 Food Sci 72:140–143. doi: 10.1111/j.1750-3841.2007.00347.x

1038 Rook GA (2013) Regulation of the immune system by biodiversity from the natural
1039 environment: An ecosystem service essential to health. Proc Natl Acad Sci 110:18360–
1040 18367. doi: 10.1073/pnas.1313731110

1041 Rook GAW (2010) 99th Dahlem Conference on Infection, Inflammation and Chronic
1042 Inflammatory Disorders: Darwinian medicine and the “hygiene” or “old friends”
1043 hypothesis. Clin Exp Immunol 160:70–79. doi: 10.1111/j.1365-2249.2010.04133.x

1044 Rook GAW (2009) Review series on helminths, immune modulation and the hygiene hypothesis:
1045 The broader implications of the hygiene hypothesis. Immunology 126:3–11. doi:
1046 10.1111/j.1365-2567.2008.03007.x

1047 Rook GAW, Hamelmann E, Rosa Brunet L (2007) Mycobacteria and allergies. Immunobiology
1048 212:461–473. doi: 10.1016/j.imbio.2007.03.003

1049 Rook GAW, Rosa Brunet L (2002) Give us this day our daily germs. Biologist (London)
1050 49:145–149

1051 Rosa Brunet L, Rook G (2008) United States Patent Application No. US 2008/0004341 A1.
1052 Retrieved from https://patents.google.com/patent/US20080004341

1053 Rusinova I, Forster S, Yu S, et al (2013) INTERFEROME v2.0: An updated database of
1054 annotated interferon-regulated genes. Nucleic Acids Res 41:. doi: 10.1093/nar/gks1215

1055 Sasso O, Russo R, Vitiello S, et al (2012) Implication of allopregnanolone in the antinociceptive
1056 effect of N-palmitoylethanolamide in acute or persistent pain. Pain. doi:
1057 10.1016/j.pain.2011.08.010

1058 Scheuerbrandt G, Bloch K (1962) Unsaturated fatty acids in microorganisms. J Biol Chem
1059 237:2064–2069

1060 Shacter E, Arzadon GK, Williams JA (1993) Stimulation of interleukin-6 and prostaglandin E2
1061 secretion from peritoneal macrophages by polymers of albumin. 82:2853–2864

1062 Smythies LE, Sellers M, Clements RH, et al (2005) Human intestinal macrophages display
1063 profound inflammatory anergy despite avid phagocytic and bacteriocidal activity. J Clin
1064 Invest 115:66–75. doi: 10.1172/JCI200519229

1065 Smythies LE, Shen R, Bimczok D, et al (2010) Inflammation anergy in human intestinal
1066 macrophages is due to Smad-induced IκBα expression and NF-κB inactivation. J Biol Chem
1067 285:19593–19604. doi: 10.1074/jbc.M109.069955

1068 Soroosh P, Doherty TA, Duan W, et al (2013) Lung-resident tissue macrophages generate Foxp3
1069 $^{+}$ regulatory T cells and promote airway tolerance. J Exp Med 210:775–788. doi:
1070 10.1084/jem.20121849

1071 Springer B, Kirschner P, Rost-Meyer G, et al (1993) *Mycobacterium interjectum*, a new species
1072 isolated from a patient with chronic lymphadenitis. J Clin Microbiol 31:3083–3089

1073 Stamper CE, Hoisington AJ, Gomez OM, et al (2016) The microbiome of the built environment
1074 and human behavior: implications for emotional health and well-being in postmodern
1075 western societies. Int Rev Neurobiol 131:289–323. doi: 10.1016/bs.irn.2016.07.006

1076 Strickland D, Kees UR, Holt PG (1996) Regulation of T-cell activation in the lung: isolated lung
1077 T cells exhibit surface phenotypic characteristics of recent activation including down-
1078 modulated T-cell receptors, but are locked into the G0/G1 phase of the cell cycle.

Immunology 87:242–249

Suutari M, Laakso S (1993) The effect of growth temperature on the fatty acid composition of *Mycobacterium phlei*. Arch Microbiol 159:119–123

Szatmari I, Pap A, Rühl R, et al (2006) PPARgamma controls CD1d expression by turning on retinoic acid synthesis in developing human dendritic cells. J Exp Med 203:2351–2362. doi: 10.1084/jem.20060141

Tay STL, Hemond HF, Polz MF, et al (1998) Two new Mycobacterium strains and their role in toluene degradation in a contaminated stream. Appl Environ Microbiol 64:1715–1720. doi: 0099-2240/98/$04.00+0

Travar M, Petkovic M, Verhaz A (2016) Type I, II, and III Interferons: Regulating Immunity to *Mycobacterium tuberculosis* Infection. Arch. Immunol. Ther. Exp. (Warsz).

Verme JL, Fu J, Astarita G, et al (2005) The Nuclear Receptor Peroxisome Proliferator-Activated Receptor- Mediates the Anti-Inflammatory Actions of Palmitoylethanolamide. Mol Pharmacol 67:15–19. doi: 10.1124/mol.104.006353

Vichai V, Kirtikara K (2006) Sulforhodamine B colorimetric assay for cytotoxicity screening. Nat Protoc 1:1112–1116. doi: 10.1038/nprot.2006.179

Watkins LR, Maier SF, Goehler LE (1995) Cytokine-to-brain communication: A review & analysis of alternative mechanisms. Life Sci.

Wollenberg GK, DeForge LE, Bolgos G, Remick DG (1993) Differential expression of tumor necrosis factor and interleukin-6 by peritoneal macrophages in vivo and in culture. Am J Pathol 143:1121–1130

Xu J, Storer PD, Chavis JA, et al (2005) Agonists for the peroxisome proliferator-activated receptor-α and the retinoid X receptor inhibit inflammatory responses of microglia. J Neurosci Res 81:403–411. doi: 10.1002/jnr.20518

Yu HL, Deng XQ, Li YJ, et al (2011) N-palmitoylethanolamide, an endocannabinoid, exhibits antidepressant effects in the forced swim test and the tail suspension test in mice. Pharmacol Reports. doi: 10.1016/S1734-1140(11)70596-5

Zhang X, Goncalves R, Mosser DM (2008) The Isolation and Characterization of Murine Macrophages. Curr Protoc Immunol CHAPTER 14: doi: 10.1002/0471142735.im1401s83.The

Zuany-Amorim C, Sawicka E, Manlius C, et al (2002) Suppression of airway eosinophilia by killed *Mycobacterium vaccae*-induced allergen-specific regulatory T-cells. Nat Med 8:625–629. doi: 10.1038/nm0602-625

FIGURE 1

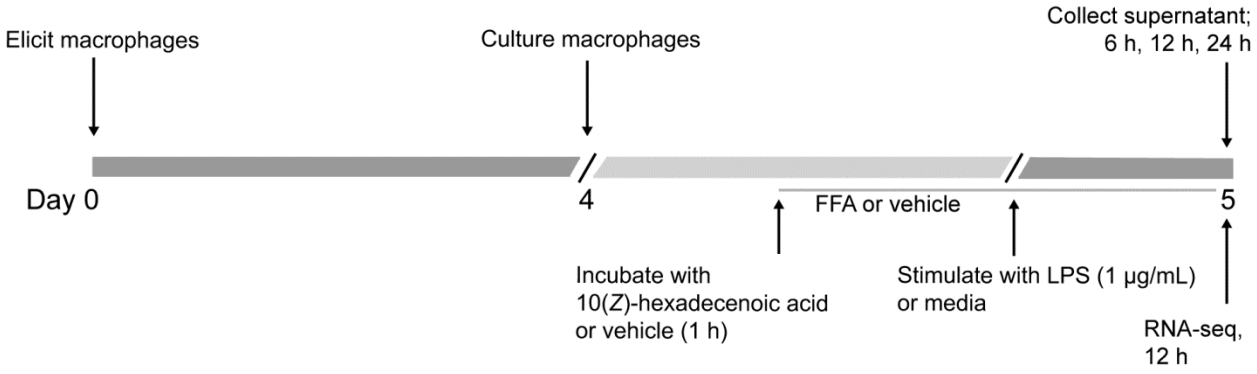
Elicit macrophages
Culture macrophages
Collect supernatant;
6 h, 12 h, 24 h
Day 0
4
5
FFA or vehicle
Incubate with
10(Z)-hexadecenoic acid
or vehicle (1 h)
Stimulate with LPS (1 µg/mL)
or media
RNA-seq,
12 h

FIGURE 2

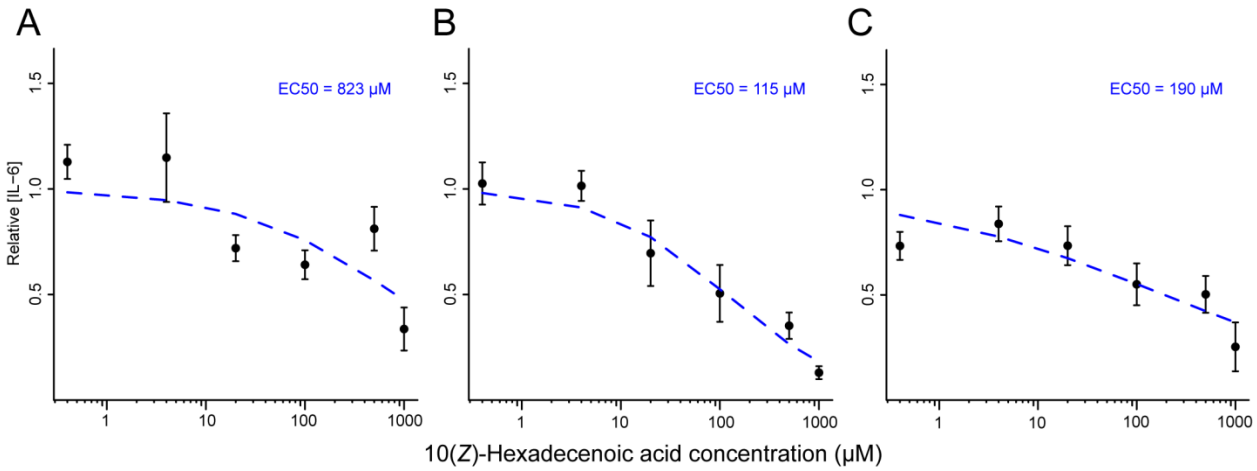
A
B
C
EC50 = 823 µM
EC50 = 115 µM
EC50 = 190 µM
Relative [IL−6]
0.5
1.0
1.5
1
10
100
1000
10(Z)-Hexadecenoic acid concentration (µM)

FIGURE 3

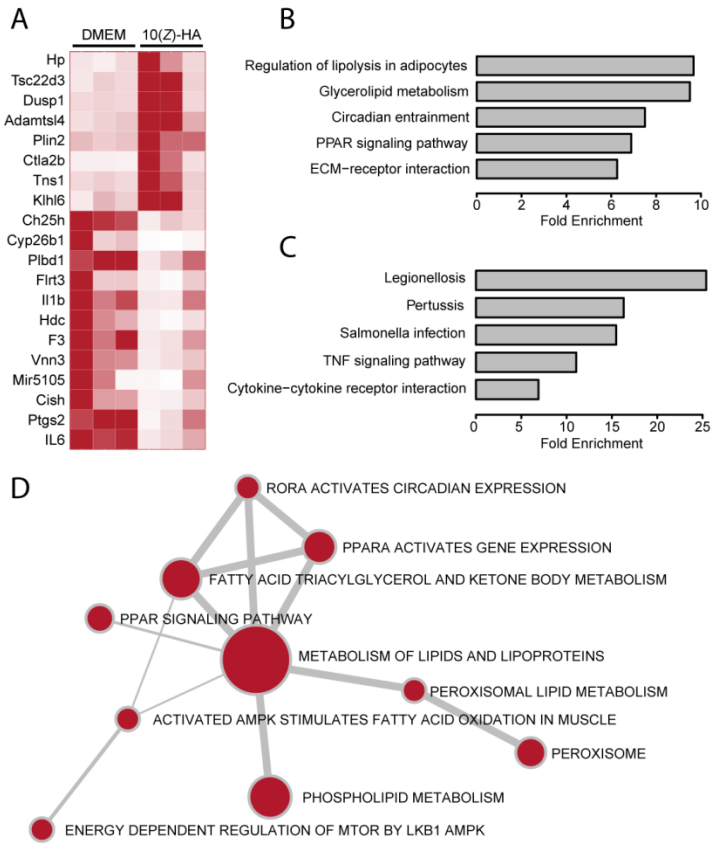
A
DMEM
10(Z)-HA
Hp
Tsc22d3
Dusp1
Adamtsl4
Plin2
Ctla2b
Tns1
Klhl6
Ch25h
Cyp26b1
Plbd1
Flrt3
Il1b
Hdc
F3
Vnn3
Mir5105
Cish
Ptgs2
IL6
B
Regulation of lipolysis in adipocytes
Glycerolipid metabolism
Circadian entrainment
PPAR signaling pathway
ECM−receptor interaction
0 2 4 6 8 10
Fold Enrichment
C
Legionellosis
Pertussis
Salmonella infection
TNF signaling pathway
Cytokine−cytokine receptor interaction
0 5 10 15 20 25
Fold Enrichment
D
RORA ACTIVATES CIRCADIAN EXPRESSION
PPARA ACTIVATES GENE EXPRESSION
FATTY ACID TRIACYLGLYCEROL AND KETONE BODY METABOLISM
PPAR SIGNALING PATHWAY
METABOLISM OF LIPIDS AND LIPOPROTEINS
PEROXISOMAL LIPID METABOLISM
ACTIVATED AMPK STIMULATES FATTY ACID OXIDATION IN MUSCLE
PEROXISOME
PHOSPHOLIPID METABOLISM
ENERGY DEPENDENT REGULATION OF MTOR BY LKB1 AMPK

FIGURE 4

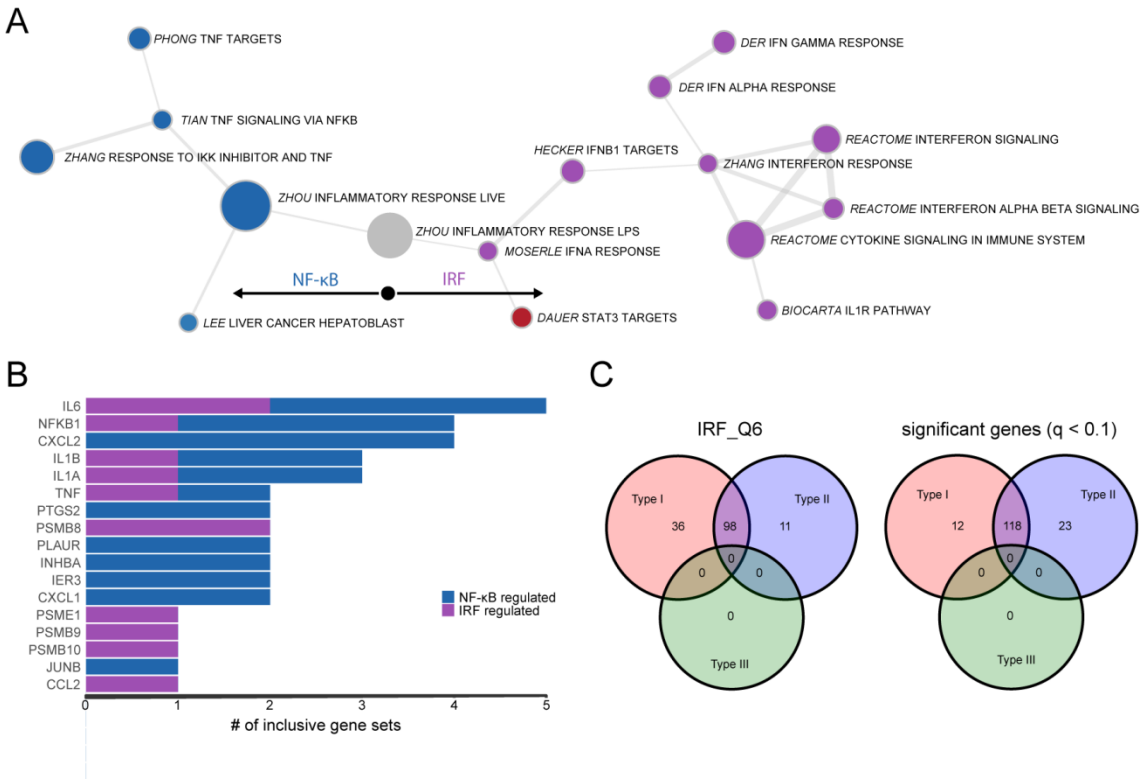
A
PHONG TNF TARGETS
TIAN TNF SIGNALING VIA NFKB
ZHANG RESPONSE TO IKK INHIBITOR AND TNF
ZHOU INFLAMMATORY RESPONSE LIVE
ZHOU INFLAMMATORY RESPONSE LPS
MOSERLE IFNA RESPONSE
LEE LIVER CANCER HEPATOBLAST
DAUER STAT3 TARGETS
NF-κB
IRF
DER IFN GAMMA RESPONSE
DER IFN ALPHA RESPONSE
HECKER IFNB1 TARGETS
ZHANG INTERFERON RESPONSE
REACTOME INTERFERON SIGNALING
REACTOME INTERFERON ALPHA BETA SIGNALING
REACTOME CYTOKINE SIGNALING IN IMMUNE SYSTEM
BIOCARTA IL1R PATHWAY
B
IL6
NFKB1
CXCL2
IL1B
IL1A
TNF
PTGS2
PSMB8
PLAUR
INHBA
IER3
CXCL1
PSME1
PSMB9
PSMB10
JUNB
CCL2
NF-κB regulated
IRF regulated
0
1
2
3
4
5
# of inclusive gene sets
C
IRF_Q6
Type I
Type II
Type III
36
98
11
0
0
0
0
significant genes (q < 0.1)
Type I
Type II
Type III
12
118
23
0
0
0
0

FIGURE 5

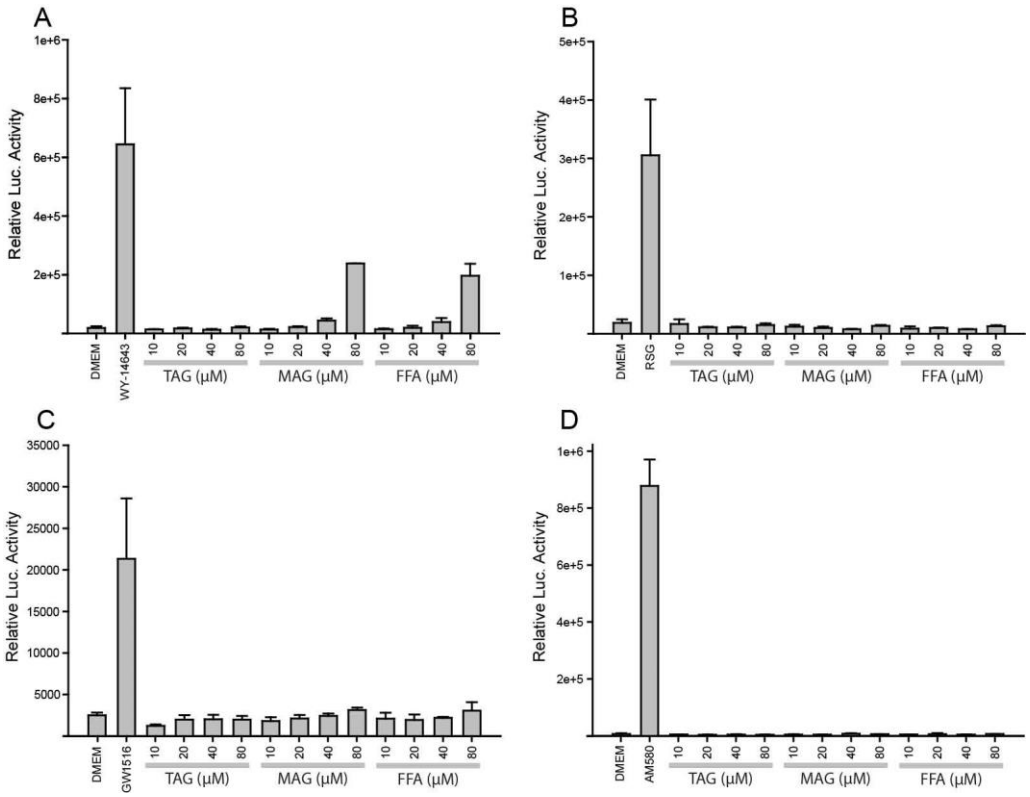
A
Relative Luc. Activity
1e+6
8e+5
6e+5
4e+5
2e+5
DMEM
WY-14643
10 20 40 80 10 20 40 80 10 20 40 80
TAG (μM)
MAG (μM)
FFA (μM)
B
Relative Luc. Activity
5e+5
4e+5
3e+5
2e+5
1e+5
DMEM
RSG
10 20 40 80 10 20 40 80 10 20 40 80
TAG (μM)
MAG (μM)
FFA (μM)
C
Relative Luc. Activity
35000
30000
25000
20000
15000
10000
5000
DMEM
GW1516
10 20 40 80 10 20 40 80 10 20 40 80
TAG (μM)
MAG (μM)
FFA (μM)
D
Relative Luc. Activity
1e+6
8e+5
6e+5
4e+5
2e+5
DMEM
AM580
10 20 40 80 10 20 40 80 10 20 40 80
TAG (μM)
MAG (μM)
FFA (μM)

FIGURE 6

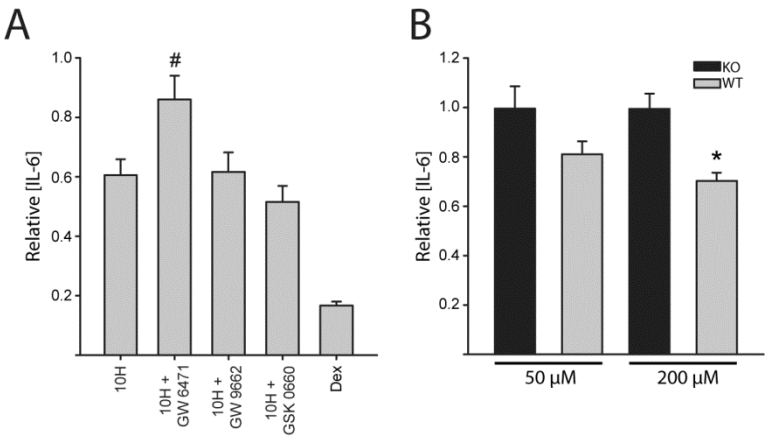
A
B
Relative [IL-6]
#
10H
10H + GW 6471
10H + GW 9662
10H + GSK 0660
Dex
KO
WT
*
50 µM
200 µM

SUPPLEMENTAL MATERIAL

Supplemental Tables

Table S1. **Dose- and time-dependent effects of 10(*Z*)-hexadecenoic acid on secretion of IL-6 from freshly isolated murine peritoneal macrophages stimulated with lipopolysaccharide.**

Concentration	P-values[1]					
	6h		12h		24h	
	LMER	*t*-test	LMER	*t*-test	LMER	*t*-test
0.4	0.45488	0.1957	0.97506	0.6117	0.172346	0.08114
4	0.12283	0.2779	0.754265	0.4239	0.810008	0.07019
20	0.16382	0.04546*	0.011331*	0.07472	0.096179	0.103
100	0.0616	0.03446*	0.000424***	0.02735*	0.00377**	0.03797*
500	0.62085	0.1786	0.000159***	0.0195*	0.003926**	0.032*
1000	0.01311*	0.002494**	2.12E-05***	0.01586*	0.000405***	0.028502*

Statistical tests consisted of pairwise comparisons of raw IL-6 values relative to paired media control values at the same time point ($n = 6$ per group). *$p < 0.05$, **$p < 0.01$, ***$p < 0.001$, two-tailed LMER or Student's *t*-test. [1]Abbreviations: LMER, linear mixed effects in R.

Table S2. Descriptive statistics of cDNA libraries and RNA-sequencing.

Sample	Library Conc. (nM)	Avg. frag. length (bp)	counts (M)
DMEM(1)	144.9	378	56.6
DMEM(2)	121	411	60.8
DMEM(3)	204.6	394	47.4
10H(1)	246	388	51.4
10H(2)	280.9	402	62.8
10H(3)	249.6	404	63.6

Abbreviations: 10H, 10(*Z*)-hexadecenoic acid; DMEM, Dulbecco's Modified Eagle Medium (DMEM)/F-12

Table S3. List of 203 differentially expressed genes between treatment with 10(*Z*)-hexadecenoic acid and vehicle in LPS-stimulated macrophages (FDR-adjusted $p < 0.1$).

Log2Fold Change	padj	gene	Ensembl ID	Log2Fold Change	padj	gene	
2.155269	2.26E-21	Hp	ENSMUSG00000031722	4.175519	0.006465	Gm807	ENSMUSG00000097848
-2.09473	4.37E-19	Il6	ENSMUSG00000025746	0.866752	0.006465	Cpt1a	ENSMUSG00000024900
2.132848	3.67E-17	Tsc22d3	ENSMUSG00000031431	1.201891	0.006658	Havcr2	ENSMUSG00000020399
-1.81185	8.08E-16	Ptgs2	ENSMUSG00000032487	-0.84047	0.006831	Zyx	ENSMUSG00000029860
-2.30575	4.38E-15	Cish	ENSMUSG00000032578	1.679239	0.006937	Wee1	ENSMUSG00000031016
1.986963	1.67E-14	Dusp1	ENSMUSG00000024190	1.318917	0.007903	Adrb2	ENSMUSG00000045730
2.012712	1.86E-12	Adamtsl4	ENSMUSG00000015850	-1.02689	0.008108	Timp1	ENSMUSG00000001131
-1.6455	1.98E-12	Mir5105	ENSMUSG00000093077	1.166393	0.008496	Foxred2	ENSMUSG00000016552
-2.04621	2.63E-12	Vnn3	ENSMUSG00000020010	1.245321	0.009034	Jdp2	ENSMUSG00000034271
1.578041	2.63E-12	Plin2	ENSMUSG00000028494	-0.8805	0.009042	Pim1	ENSMUSG00000024014
-1.93629	5.09E-12	F3	ENSMUSG00000028128	0.881662	0.009058	Sgms1	ENSMUSG00000040451
-2.8558	5.31E-12	Hdc	ENSMUSG00000027360	1.272806	0.00933	Rims3	ENSMUSG00000032890
-1.5767	6.48E-12	Il1b	ENSMUSG00000027398	0.915219	0.009572	Prkar2b	ENSMUSG00000002997
-2.15506	7.97E-12	Flrt3	ENSMUSG00000051379	-1.60497	0.009607	Rnf180	ENSMUSG00000021720
3.024984	2.40E-11	Ctla2b	ENSMUSG00000074874	-2.14325	0.009652	Syt7	ENSMUSG00000024743
1.811323	4.79E-11	Tns1	ENSMUSG00000055322	-1.6082	0.009895	Hspa1a	ENSMUSG00000091971
1.82332	1.45E-10	Klhl6	ENSMUSG00000043008	-1.02922	0.010112	Tfec	ENSMUSG00000029553
-1.53809	2.78E-10	Plbd1	ENSMUSG00000030214	-1.32561	0.010112	Zfp558	ENSMUSG00000074500
-4.06225	4.95E-10	Cyp26b1	ENSMUSG00000063415	-0.78966	0.010112	Il1rn	ENSMUSG00000026981

-2.35715	5.70E-10	Ch25h	ENSMUSG00000050370	0.801393	0.010902	Dock10	ENSMUSG00000038608
-1.4212	3.35E-09	Ccl7	ENSMUSG00000035373	0.858932	0.010902	Tgfbi	ENSMUSG00000035493
-1.34039	4.91E-09	Ccl2	ENSMUSG00000035385	0.788151	0.010902	Pla2g7	ENSMUSG00000023913
-3.35822	6.81E-09	Car4	ENSMUSG00000000805	1.794042	0.010902	Srgap3	ENSMUSG00000030257
1.750436	1.16E-08	Susd2	ENSMUSG00000006342	0.983421	0.010993	Abcc3	ENSMUSG00000020865
-3.51502	2.92E-08	Adm	ENSMUSG00000030790	-1.03832	0.012028	Dennd3	ENSMUSG00000036661
-1.41666	4.57E-08	Il12a	ENSMUSG00000027776	0.78379	0.013193	Man2a1	ENSMUSG00000024085
1.394626	5.98E-08	Ppp1r12b	ENSMUSG00000073557	1.561095	0.013193	Frmd4b	ENSMUSG00000030064
1.317669	7.23E-08	Dennd4c	ENSMUSG00000038024	1.181418	0.013404	Per2	ENSMUSG00000055866
-1.56573	7.86E-08	Gm10499	ENSMUSG00000073403	1.920189	0.013773	Kcnk13	ENSMUSG00000045404
-1.76168	1.01E-07	Hbegf	ENSMUSG00000024486	-0.80185	0.014517	Plk2	ENSMUSG00000021701
1.619779	2.04E-07	Ms4a8a	ENSMUSG00000024730	1.39729	0.014584	Nrg4	ENSMUSG00000032311
-1.29736	2.22E-07	Itgax	ENSMUSG00000030789	1.946616	0.016015	Fabp4	ENSMUSG00000062515
-1.48148	3.26E-07	Ccl22	ENSMUSG00000031779	0.814942	0.018239	Adam8	ENSMUSG00000025473
1.312963	5.18E-07	Glul	ENSMUSG00000026473	-0.99463	0.018957	Slamf1	ENSMUSG00000015316
-1.29094	6.75E-07	Iigp1	ENSMUSG00000054072	0.896952	0.01948	Plpp1	ENSMUSG00000021759
1.426376	7.14E-07	Lpxn	ENSMUSG00000024696	0.778795	0.01948	Cd47	ENSMUSG00000055447
-1.30554	8.49E-07	Slc1a2	ENSMUSG00000005089	3.257959	0.019865	Saxo1	ENSMUSG00000028492
1.555412	8.59E-07	Fos	ENSMUSG00000021250	-2.11589	0.023245	Csf2	ENSMUSG00000018916
-1.73463	1.06E-06	Scimp	ENSMUSG00000057135	-0.83357	0.024354	Gm14023	ENSMUSG00000085498
1.307021	1.18E-06	Slc43a2	ENSMUSG00000038178	1.256371	0.026556	Cdo1	ENSMUSG00000033022
2.671207	1.26E-06	Ly6c2	ENSMUSG00000022584	-0.81499	0.027117	Ier3	ENSMUSG00000003541
1.168314	2.02E-06	Lcn2	ENSMUSG00000026822	0.806704	0.029122	Dock5	ENSMUSG00000044447
1.578367	2.97E-06	Fkbp5	ENSMUSG00000024222	-0.71877	0.029122	Ccl3	ENSMUSG00000000982
1.370214	4.86E-06	Sepp1	ENSMUSG00000064373	0.851011	0.03319	Rassf2	ENSMUSG00000027339
1.299991	5.32E-06	Sort1	ENSMUSG00000068747	-1.53448	0.03319	Schip1	ENSMUSG00000027777
-1.24524	1.79E-05	Upp1	ENSMUSG00000020407	0.943748	0.034299	Alox5ap	ENSMUSG00000060063

-1.1367	2.36E-05	Ccl6	ENSMUSG00000018927	0.738488	0.039546	Sdc4	ENSMUSG00000017009
-1.35404	2.68E-05	Cnn3	ENSMUSG00000053931	-1.05575	0.043357	Olfm1	ENSMUSG00000026833
-2.22194	2.86E-05	Gm5483	ENSMUSG00000079597	0.734737	0.044388	Mt2	ENSMUSG00000031762
1.131171	3.65E-05	Ecm1	ENSMUSG00000028108	-0.71991	0.044388	Inhba	ENSMUSG00000041324
1.297072	3.65E-05	Cacna1d	ENSMUSG00000015968	0.833112	0.044388	Ift57	ENSMUSG00000032965
-1.28314	3.90E-05	Olr1	ENSMUSG00000030162	1.775472	0.044388	Fabp7	ENSMUSG00000019874
-1.54507	4.24E-05	Ahr	ENSMUSG00000019256	-0.78572	0.044388	Trim30c	ENSMUSG00000078616
-1.96156	4.34E-05	Car2	ENSMUSG00000027562	-0.68344	0.044485	Rpph1	ENSMUSG00000092837
-2.66361	5.55E-05	Hspa1b	ENSMUSG00000090877	0.75981	0.047915	Ezr	ENSMUSG00000052397
-1.0926	6.25E-05	Plaur	ENSMUSG00000046223	-0.87194	0.048952	Cd83	ENSMUSG00000015396
-1.22776	7.12E-05	Procr	ENSMUSG00000027611	0.802102	0.048952	Gpcpd1	ENSMUSG00000027346
1.463418	8.54E-05	Nav2	ENSMUSG00000052512	-0.72003	0.050936	Nfkb2	ENSMUSG00000025225
-1.03592	0.000104	Tnf	ENSMUSG00000024401	-1.8997	0.050936	Lrrc32	ENSMUSG00000090958
-1.12432	0.000105	Serpinb2	ENSMUSG00000062345	0.746734	0.051435	Itga4	ENSMUSG00000027009
-1.08005	0.000134	Clec7a	ENSMUSG00000079293	-0.92303	0.051789	Cd86	ENSMUSG00000022901
-3.0819	0.000134	Ccl17	ENSMUSG00000031780	-0.73811	0.051789	Cmklr1	ENSMUSG00000042190
2.207158	0.000208	Orm1	ENSMUSG00000039196	-1.11436	0.051885	Il12b	ENSMUSG00000004296
1.323308	0.000232	Cd300a	ENSMUSG00000034652	-1.98017	0.053401	Gm13872	ENSMUSG00000087185
0.972281	0.00028	Saa3	ENSMUSG00000040026	0.784546	0.056288	Gm12840	ENSMUSG00000086320
-1.20636	0.000281	Egr2	ENSMUSG00000037868	-0.70065	0.05698	Oasl1	ENSMUSG00000041827
-0.95987	0.000319	Il1a	ENSMUSG00000027399	-0.70774	0.05698	Irf8	ENSMUSG00000041515
-1.62852	0.00032	Tnc	ENSMUSG00000028364	-1.19175	0.058415	Frmd6	ENSMUSG00000048285
1.004165	0.000329	Xdh	ENSMUSG00000024066	0.849896	0.058415	Per1	ENSMUSG00000020893
-0.97547	0.000451	Cmpk2	ENSMUSG00000020638	0.735235	0.059193	Hal	ENSMUSG00000020017
1.213513	0.000585	Htra1	ENSMUSG00000006205	-0.72158	0.059548	Wars	ENSMUSG00000021266
-1.53878	0.000656	Irf4	ENSMUSG00000021356	1.006913	0.062477	Mmp19	ENSMUSG00000025355
-1.42269	0.000656	AA467197	ENSMUSG00000033213	-0.57969	0.062658	Gm10800	ENSMUSG00000075014

-2.07631	0.000696	Kazn	ENSMUSG00000040606	-0.67963	0.065954	Nos2	ENSMUSG00000020826
0.956982	0.000867	Cd24a	ENSMUSG00000047139	-0.83535	0.066479	Csrnp1	ENSMUSG00000032515
-0.89122	0.000958	Rmrp	ENSMUSG00000088088	0.712094	0.068155	Gm26809	ENSMUSG00000097815
-0.9802	0.001016	Ccl4	ENSMUSG00000018930	-0.78044	0.068155	Insig1	ENSMUSG00000045294
3.903311	0.001194	Dnah12	ENSMUSG00000021879	-0.61444	0.070733		ENSMUSG00000045999
1.169473	0.001524	Rin3	ENSMUSG00000044456	1.704424	0.071129	Bpifc	ENSMUSG00000050108
1.169244	0.001741	F13a1	ENSMUSG00000039109	0.701972	0.071129	Pdxk	ENSMUSG00000032788
-0.949	0.002022	Chst11	ENSMUSG00000034612	0.994597	0.071577	Trim29	ENSMUSG00000032013
-0.9961	0.002166	Casp7	ENSMUSG00000025076	-0.8871	0.076468	Mmp13	ENSMUSG00000050578
3.931076	0.002435	Bach2os	ENSMUSG00000086150	0.991755	0.078103	Wipi1	ENSMUSG00000041895
0.885144	0.002435	Lox	ENSMUSG00000024529	1.00311	0.079388	Serinc5	ENSMUSG00000021703
-1.66375	0.002486	Rhoh	ENSMUSG00000029204	-1.25174	0.079543	Il1f9	ENSMUSG00000044103
-1.24964	0.002515		ENSMUSG00000092773	-0.67556	0.080434	Nfkb1	ENSMUSG00000028163
-1.08726	0.002887	Socs1	ENSMUSG00000038037	0.942972	0.080838	Syt11	ENSMUSG00000068923
1.302178	0.003251	Paqr7	ENSMUSG00000037348	1.324205	0.080838	Klra2	ENSMUSG00000030187
-0.90079	0.003254	Mmp12	ENSMUSG00000049723	-0.71767	0.082101	Tmem2	ENSMUSG00000024754
-1.06355	0.003509	Csf3	ENSMUSG00000038067	0.734669	0.082101	Ergic1	ENSMUSG00000001576
-2.35111	0.003653	Il11	ENSMUSG00000004371	-0.80694	0.08253	Wfs1	ENSMUSG00000039474
-0.84287	0.003941	Rsad2	ENSMUSG00000020641	-0.68387	0.082531	Isg15	ENSMUSG00000035692
-1.12922	0.004208	Timp3	ENSMUSG00000020044	-0.67778	0.083148	Cxcl3	ENSMUSG00000029379
-2.03218	0.004208	Dcstamp	ENSMUSG00000022303	-0.90013	0.086117	Fst	ENSMUSG00000021765
1.386263	0.00424	Mgll	ENSMUSG00000033174	1.157447	0.087469	Apoc2	ENSMUSG00000002992
-0.89309	0.004485	Dab2	ENSMUSG00000022150	0.80021	0.090822	Cyth3	ENSMUSG00000018001
1.14163	0.005073	Mafb	ENSMUSG00000028874	1.07939	0.090822	Col18a1	ENSMUSG00000001435
0.940402	0.005073	Fgr	ENSMUSG00000074622	-1.25793	0.091248	Osmr	ENSMUSG00000022146
-0.81843	0.006355	Cxcl2	ENSMUSG00000058427	-1.42935	0.091568	Alpk2	ENSMUSG00000032845
-1.24059	0.006465	Ptgs2os2	ENSMUSG00000097754	-0.72425	0.09327	Axl	ENSMUSG00000002602

				0.815505	0.095702	Aldh9a1	ENSMUSG00000026687
				0.925759	0.095702	Cav1	ENSMUSG00000007655
				3.350338	0.099786	Glyctk	ENSMUSG00000020258

1210

1211

1212

1213

1214

1215

1216

1217

1218

1219

1220

1221

1222

Table S4. KEGG pathways and GO biological processes with associated genes that are significantly downregulated in LPS-stimulated murine macrophages preincubated with 10(Z)-hexadecenoic acid, relative to LPS-stimulated murine macrophages preincubated with media.

NF-κB (KEGG PATHWAY: mmu04064)	**Jak-STAT (KEGG PATHWAY: mmu04630)**	**Inflammatory response (GO:0006954)**	
chemokine (C-C motif) ligand 4 (Ccl4)	colony stimulating factor 2 (granulocyte-macrophage)(Csf2)	AXL receptor tyrosine kinase (Axl)	chemokine (C-X-C motif) ligand 3 (Cxcl3)
interleukin 1 beta (Il1b)	colony stimulating factor 3 (granulocyte) (Csf3)	C-type lectin domain family 7, member a (Clec7a)	cytochrome P450, family 26, subfamily b, polypeptide 1 (Cyp26b1)
nuclear factor of kappa light polypeptide gene enhancer in B cells 1, p105 (Nfkb1)	cytokine inducible SH2-containing protein (Cish)	chemokine (C-C motif) ligand 17 (Ccl17)	interleukin 1 alpha (Il1a)
nuclear factor of kappa light polypeptide gene enhancer in B cells 2, p49/p100 (Nfkb2)	interleukin 11 (Il11)	chemokine (C-C motif) ligand 2 (Ccl2)	interleukin 1 beta (Il1b)
prostaglandin-endoperoxide synthase 2 (Ptgs2)	interleukin 12a (Il12a)	chemokine (C-C motif) ligand 22 (Ccl22)	interleukin 1 family, member 9 (Il1f9)
tumor necrosis factor (Tnf)	interleukin 12b (Il12b)	chemokine (C-C motif) ligand 3 (Ccl3)	interleukin 6 (Il6)
	interleukin 6 (Il6)	chemokine (C-C motif) ligand 4 (Ccl4)	nitric oxide synthase 2, inducible (Nos2)
	oncostatin M receptor (Osmr)	chemokine (C-C motif) ligand 6 (Ccl6)	nuclear factor of kappa light polypeptide gene

			enhancer in B cells 2, p49/p100 (Nfkb2)
	proviral integration site 1 (Pim1)	chemokine (C-C motif) ligand 7 (Ccl7)	oxidized low density lipoprotein (lectin-like) receptor 1 (Olr1)
	suppressor of cytokine signaling 1(Socs1)	chemokine (C-X-C motif) ligand 2(Cxcl2)	prostaglandin-endoperoxide synthase 2 (Ptgs2)
			tumor necrosis factor (Tnf)

Table S5. Top scoring KEGG pathways enriched for differentially expressed genes (q < 0.1).

Term	Count	% genes in pathway	Fold Enrichment	Benjamini	FDR

mmu05134:Legionellosis	12	6.185567	15.33267	3.36E-08	2.33E-07
mmu05133:Pertussis	11	5.670103	10.82611	4.33E-06	6.01E-05
mmu05132:Salmonella infection	11	5.670103	10.27092	4.83E-06	1.01E-04
mmu05140:Leishmaniasis	10	5.154639	11.37972	7.38E-06	2.05E-04
mmu05323:Rheumatoid arthritis	10	5.154639	8.88173	5.13E-05	0.001779
mmu04668:TNF signaling pathway	11	5.670103	7.349836	5.77E-05	0.002402
mmu04620:Toll-like receptor signaling pathway	10	5.154639	7.21091	2.11E-04	0.010234
mmu05142:Chagas disease (American trypanosomiasis)	10	5.154639	7.070892	2.17E-04	0.012025
mmu04640:Hematopoietic cell lineage	9	4.639175	7.803235	3.27E-04	0.020396
mmu04060:Cytokine-cytokine receptor interaction	14	7.216495	4.161725	4.43E-04	0.030737
mmu05164:Influenza A	11	5.67010	4.684983	0.001651	0.12604

		3			3
mmu05321:Inflammatory bowel disease (IBD)	7	3.608247	8.64087	0.00203	0.169085
mmu04630:Jak-STAT signaling pathway	10	5.154639	5.022772	0.002005	0.180893
mmu05146:Amoebiasis	9	4.639175	5.602322	0.002267	0.220249
mmu04062:Chemokine signaling pathway	11	5.670103	4.087409	0.003697	0.384834
mmu05144:Malaria	6	3.092784	9.103774	0.005023	0.557603
mmu05162:Measles	9	4.639175	4.819645	0.005203	0.613481
mmu05152:Tuberculosis	10	5.154639	4.138079	0.006105	0.761997
mmu05145:Toxoplasmosis	8	4.123711	5.15612	0.007753	1.021024
mmu05143:African trypanosomiasis	5	2.57732	10.40431	0.010775	1.492265
mmu04940:Type I diabetes mellitus	6	3.092784	7.048083	0.012405	1.802632

mmu05168:Herpes simplex infection	10	5.154639	3.501451	0.016134	2.452592
mmu05332:Graft-versus-host disease	5	2.57732	7.002903	0.040085	6.321057
mmu05205:Proteoglycans in cancer	9	4.639175	3.228925	0.045359	7.439826
mmu04621:NOD-like receptor signaling pathway	5	2.57732	6.502695	0.047851	8.154999
mmu04380:Osteoclast differentiation	7	3.608247	4.046122	0.048295	8.543908
mmu04010:MAPK signaling pathway	10	5.154639	2.878664	0.047148	8.651597
mmu04064:NF-kappa B signaling pathway	6	3.092784	4.50496	0.062425	11.772
mmu04622:RIG-I-like receptor signaling pathway	5	2.57732	5.355161	0.079744	15.40049
mmu00910:Nitrogen metabolism	3	1.546392	12.85239	0.122031	23.7337
mmu05330:Allograft rejection	4	2.061856	5.202156	0.209372	39.67281
mmu00340:Histidine metabolism	3	1.54639	9.103774	0.209628	40.6909

		2			
mmu04923:Regulation of lipolysis in adipocytes	4	2.061856	5.11089	0.206209	41.0717
mmu04915:Estrogen signaling pathway	5	2.57732	3.715826	0.209529	42.5792
mmu04623:Cytosolic DNA-sensing pathway	4	2.061856	4.551887	0.253222	50.79551
mmu04932:Non-alcoholic fatty liver disease (NAFLD)	6	3.092784	2.783319	0.271611	54.69423
mmu05020:Prion diseases	3	1.546392	6.82783	0.29259	58.88365
mmu04917:Prolactin signaling pathway	4	2.061856	3.990695	0.310953	62.54923
mmu05410:Hypertrophic cardiomyopathy (HCM)	4	2.061856	3.687604	0.355616	69.55837
mmu03320:PPAR signaling pathway	4	2.061856	3.641509	0.357001	70.64847

Table S6. Top scoring KEGG pathway enrichment scores of 10(*Z*)-hexadecenoic acid treatment.

NAME	SIZE	ES	NES	NOM p-val	FDR q-val	FWER p-val
KEGG_PEROXISOME	70	0.455491	1.776987	0	0.206677	0.202
KEGG_PPAR_SIGNALING_PATHWAY	50	0.405869	1.523902	0.022688	0.965135	0.877

KEGG_CITRATE_CYCLE_TCA_CYCLE	26	0.458822	1.441984	0.062157	1	0.976
KEGG_FATTY_ACID_METABOLISM	35	0.410082	1.418581	0.066784	1	0.985
KEGG_PROPANOATE_METABOLISM	29	0.381988	1.262367	0.171735	1	1

Table S7. Transcription factor binding site enrichment scores of 10(*Z*)-hexadecenoic acid treatment.

NAME	SIZE	ES	NES	NOM p-val	FDR q-val	FWER p-val
MYB_Q3	193	0.354277	1.630786	0	0.4669	0.462
CREBP1_01	138	0.353955	1.554846	0.001592	0.570198	0.79
MYB_Q5_01	199	0.327401	1.527497	0.003185	0.502861	0.861
TGATTTRY_GFI1_01	196	0.329035	1.51785	0	0.417293	0.885
PPARA_01	31	0.448403	1.497608	0.024433	0.41565	0.938

Table S8. Transcription factor binding site enrichment scores of DMEM (i.e., LPS exposure, in the absence of 10(*Z*)-hexadecenoic acid treatment).

NAME	SIZE	ES	NES	NOM p-val	FDR q-val	FWER p-val
YAATNANRNNNCAG_UNKNOWN	111	-0.38331	-1.73728	0	0.188651	0.134
GGAMTNNNNNTCCY_UNKNOWN	45	-0.45405	-1.72149	0	0.105558	0.147
NFKB_Q6_01	196	-0.34847	-1.68059	0	0.110536	0.223
NFKB_Q6	214	-0.33542	-1.63828	0	0.137538	0.345
GGCNKCCATNK_UNKNOWN	110	-0.35338	-1.56007	0.002342	0.235213	0.583
IRF_Q6	200	-0.31662	-1.53823	0.007916	0.237864	0.654
NFKB_C	216	-0.30917	-1.53386	0	0.214951	0.676
NFKAPPAB65_01	194	-0.30235	-1.46879	0.002611	0.363113	0.888
NFKAPPAB_01	210	-0.29933	-1.4586	0.002786	0.356037	0.915
IRF2_01	105	-0.32533	-1.4371	0.012019	0.39177	0.951

Table S9. Selective peroxisome proliferator-activated receptor (PPAR) antagonists and agonists.

	Antagonist		Agonist	
	Name	IC_{50}	Name	EC_{50}
PPARα	GW 6471 (Cat. No. 4618)	0.24 μM[1]	WY 14643 (Cat. No. 1312)	0.63 μM[1]
PPARγ	GW 9662 (Cat. No. 1508)	3.3 nM[1]	Rosiglitazone (Cat. No. 5325)	60 nM[1]
PPARδ	GSK 0660 (Cat. No. 3433)	0.16 μM[1]	GW 0742 (Cat. No. 2229)	1 nM[1]

[1]According to manufacturer information.

Table S10. **Lipopolysaccharide-induced proinflammatory cytokine and chemokine ligand mRNAs downregulated by preincubation of freshly isolated murine peritoneal macrophages with 10(*Z*)-hexadecenoic acid (selected from 203 differentially expressed mRNAs).**

#	Ensemble ID	Mean #Reads LPS (n =3)	Mean #Reads s148.2ffa +LPS (n = 3)	Fold-change	Log2 Fold-change	*p* value	Adjusted *p* value	Gene

2	ENSMUSG0000 0025746	1302	305	0.23	-2.09	4.19E-23	4.37E-19	Il6
13	ENSMUSG0000 0027398	15,957	5349	0.34	-2.16	4.03E-15	6.48E-12	Il1b
21	ENSMUSG0000 0035373	1182	441	0.37	-1.42	3.37E-12	3.35E-9	Ccl7
22	ENSMUSG0000 0035385	5656	2234	0.39	-1.34	5.18E-12	4.91E-9	Ccl2
26	ENSMUSG0000 0027776	714	268	0.37	-1.42	5.70E-11	4.57E-8	Il12a
33	ENSMUSG0000 0031779	327	117	0.36	-1.48	5.15E-10	3.26E-7	Ccl22
47	ENSMUSG0000 0018927	810	368	0.45	-1.14	5.31E-8	2.36E-5	Ccl6
59	ENSMUSG0000 0024401	2098	1023	0.49	-1.04	2.95E-7	1.04E-4	Tnf
61	ENSMUSG0000 0031780	24	3	0.12	-3.08	3.97E-7	1.34E-4	Ccl17
67	ENSMUSG0000 0027399	16533	8500	0.51	-0.96	1.02E-6	3.19E-4	Il1a
77	ENSMUSG0000 0018930	603	305	0.51	-0.98	3.75E-6	1.02E-3	Ccl4
91	ENSMUSG0000 0004371	26	5	0.20	-2.35	1.59E-5	3.7E-3	Il11
99	ENSMUSG0000 0058427	4726	2680	0.57	-0.82	3.01E-5	6.4E-3	Cxcl2[1]
142	ENSMUSG0000	6693	4067	0.61	-0.72	1.99E-	2.9E-2	Ccl3

	0000982					4		
158	ENSMUSG0000 0025225	916	556	0.61	-0.72	3.85E-4	5.09E-2	Nfkb2
161	ENSMUSG0000 0042190	789	473	0.60	-0.74	4.02E-4	5.18E-2	Cmklr1
163	ENSMUSG0000 0004296	77	35	0.46	-1.11	4.05E-4	5.19E-2	Il12b
167	ENSMUSG0000 0041515	775	475	0.61	-0.71	4.56E-4	5.70E-2	Irf8
185	ENSMUSG0000 0044103	50	21	0.42	-1.25	7.05E-4	7.95E-2	Il1f9
186	ENSMUSG0000 0028163	1109	694	0.63	-0.68	7.16E-4	8.04E-2	Nfkb1
193	ENSMUSG0000 0029379	8341	5214	0.62	-0.68	7.68E-4	8.31E-2	Cxcl3

[1]Cxcl2 is a functional homologue of human IL-8

Table S11. Significant enrichment of "immune system process" (GO: 0006955) in lipopolysaccharide-induced mRNAs downregulated by preincubation of freshly isolated murine peritoneal macrophages with 10(*Z*)-hexadecenoic acid.

Ensemble ID	**Mean #Reads LPS (n =3)**	**Mean #Reads s148.2ffa +LPS (n = 3)**	**Log2 Fold-change**	***p* value**	**Adjusted *p* value**	**Gene**
ENSMUSG00000019256	124.9318	42.81153	-1.54507	1.08E-07	4.24E-05	Ahr
ENSMUSG00000029379	8341.778	5214.664	-0.67778	0.000768	0.083148	Cxcl3
ENSMUSG00000029204	49.42187	15.5984	-1.66375	1.01E-05	0.002486	Rhoh
ENSMUSG00000041827	1097.95	675.5632	-0.70065	0.000454	0.05698	Oasl1
ENSMUSG00000041515	775.8443	475.0327	-0.70774	0.000456	0.05698	Irf8

ENSMUSG00000004296	77.84137	35.95454	-1.11436	0.000405	0.051885	Il12b
ENSMUSG00000042190	789.4998	473.3228	-0.73811	0.000402	0.051789	Cmklr1
ENSMUSG00000027398	15956.74	5349.469	-1.5767	4.03E-15	6.48E-12	Il1b
ENSMUSG00000027399	16533.28	8499.829	-0.95987	1.02E-06	0.000319	Il1a
ENSMUSG00000058427	4726.055	2679.948	-0.81843	3.01E-05	0.006355	Cxcl2
ENSMUSG00000035692	773.1049	481.2528	-0.68387	0.000759	0.082531	Isg15
ENSMUSG00000022901	143.9578	75.92354	-0.92303	0.0004	0.051789	Cd86
ENSMUSG00000018916	26.48043	6.109115	-2.11589	0.000154	0.023245	Csf2
ENSMUSG00000038067	215.195	102.9609	-1.06355	1.51E-05	0.003509	Csf3
ENSMUSG00000044103	50.60669	21.25181	-1.25174	0.000705	0.079543	Il1f9
ENSMUSG00000000982	6693.382	4066.999	-0.71877	0.000199	0.029122	Ccl3
ENSMUSG00000015316	164.228	82.4202	-0.99463	0.000122	0.018957	Slamf1
ENSMUSG00000002602	383.6876	232.2509	-0.72425	0.000893	0.09327	Axl
ENSMUSG00000054072	609.7951	249.2138	-1.29094	1.13E-09	6.75E-07	Iigp1
ENSMUSG00000022303	33.02525	8.074181	-2.03218	1.89E-05	0.004208	Dcstamp
ENSMUSG00000027776	714.3374	267.5763	-1.41666	5.7E-11	4.57E-08	Il12a
ENSMUSG00000018930	602.5693	305.4475	-0.9802	3.75E-06	0.001016	Ccl4
ENSMUSG00000021356	87.38355	30.07534	-1.53878	2.27E-06	0.000656	Irf4
ENSMUSG00000035373	1181.631	441.2235	-1.4212	3.37E-12	3.35E-09	Ccl7
ENSMUSG00000020641	2750.461	1533.472	-0.84287	1.74E-05	0.003941	Rsad2
ENSMUSG00000018927	809.8237	368.3064	-1.1367	5.31E-08	2.36E-05	Ccl6
ENSMUSG00000035385	5656.07	2233.662	-1.34039	5.18E-12	4.91E-09	Ccl2
ENSMUSG00000030789	1173.119	477.3067	-1.29736	3.41E-10	2.22E-07	Itgax
ENSMUSG00000031780	24.3371	2.874252	-3.0819	3.97E-07	0.000134	Ccl17
ENSMUSG00000030162	279.057	114.6645	-1.28314	9.71E-08	0.000039	Olr1
ENSMUSG00000031779	326.9606	117.0914	-1.48148	5.15E-10	3.26E-07	Ccl22
ENSMUSG00000025225	916.256	556.2449	-0.72003	0.000385	0.050936	Nfkb2
ENSMUSG00000050370	100.3056	19.57727	-2.35715	5.46E-13	5.7E-10	Ch25h
ENSMUSG00000026981	3855.465	2230.31	-0.78966	5.76E-05	0.010112	Il1rn
ENSMUSG00000024401	2098.107	1023.257	-1.03592	2.95E-07	0.000104	Tnf

ENSMUSG00000025746	1302.137	304.8466	-2.09473	4.19E-23	4.37E-19	Il6

1264
1265

Supplemental Figures

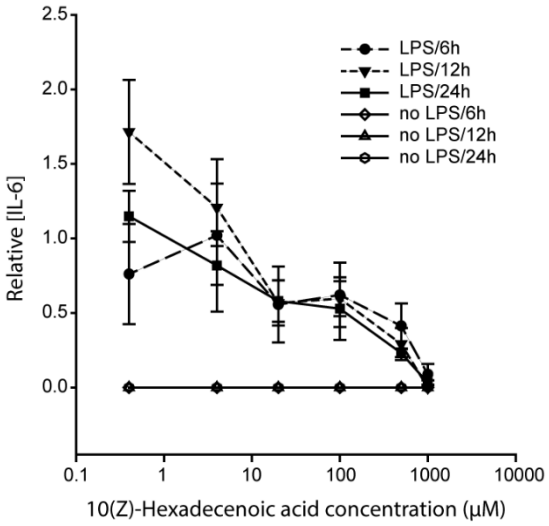

Fig. S1. 10(Z)-hexadecenoic acid alone has no detectable effect IL-6 release.

After isolation of peritoneal macrophages and incubation with 10(Z)-hexadecenoic acid for 1 h, macrophages were challenged with either lipopolysaccharide (LPS) or Dulbecco's Modified Eagle Medium (DMEM; as control). There was no detectable effect of 10(Z)-hexadecenoic acid on interleukin (IL) 6 secretion in the cultures that did not receive LPS. Abbreviations: IL-6, interleukin 6; LPS, lipopolysaccharide. Data are representative of 3 replicates per condition.

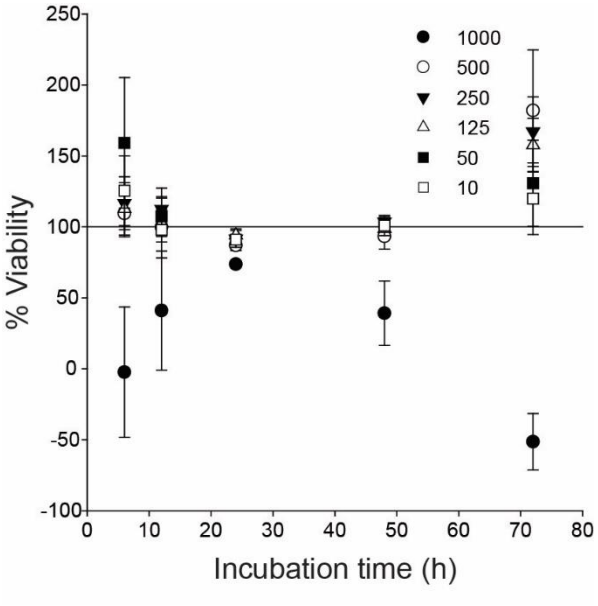

Fig. S2. Effect of 10(*Z*)-hexadecencoic acid on macrophage cell viability.

Sulforhodamine B (SRB) was used to assess cytotoxic effects of various concentrations of synthetic 10(Z)-hexadecenoic acid (10 µM, 50 µM, 125 µM, 250 µM, 500 µM, 1000 µM) after 0, 6, 12, 24, 48, and 72 h of incubation with freshly isolated murine peritoneal macrophages. Percent control growth is expressed as % viability and is a ratio of the amount of growth that occurred with treatment over the amount of growth that occurred in media. One hundred percent indicates no differences in cell growth between treatment and media, whereas values below 100% indicate that growth was impaired with treatment. Data are expressed as mean ± SEM of 3-7 mice per condition.

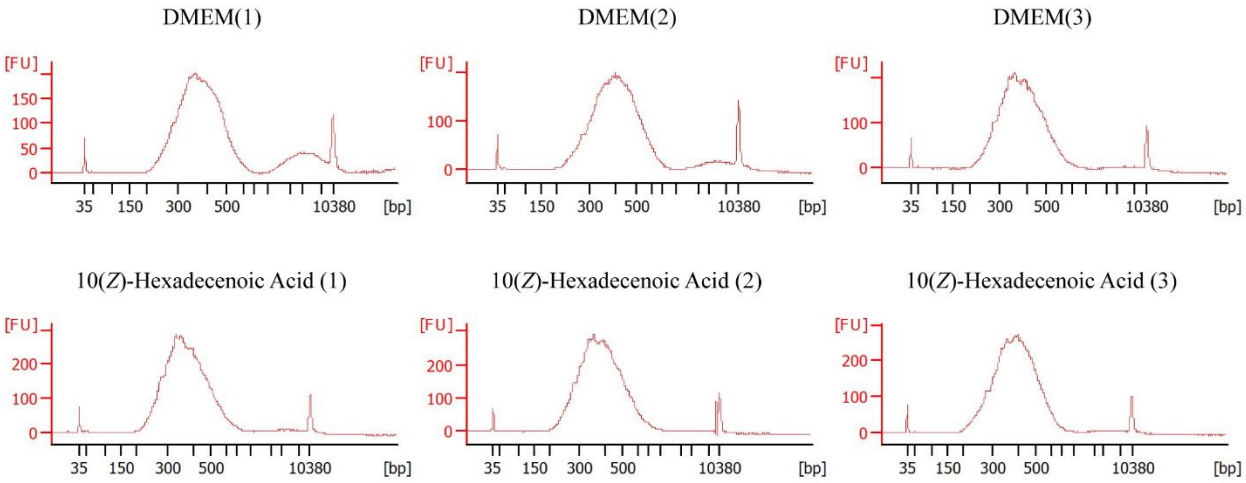

Fig. S3. BioAnalyzer electropherograms of cDNA libraries used for RNA-sequencing.

Total RNA content of $1x10^5$ macrophages was prepared for each sample utilizing separate macrophage preparations from $n = 3$ mice treated with vehicle (Dulbecco's Modified Eagle Medium (DMEM; upper row) then challenged with 1µg/mL lipopolysaccharide (LPS) or $n = 3$ mice treated with 200 µM 10(*Z*)-hexadecenoic acid for 1 h, then challenged with 1µg/mL LPS. Macrophages were harvested 12 h following LPS challenge. Peaks at 35 bp and 10,380 bp are gel migration markers. For concentrations of cDNA and average fragment length for each sample, see Table S2.

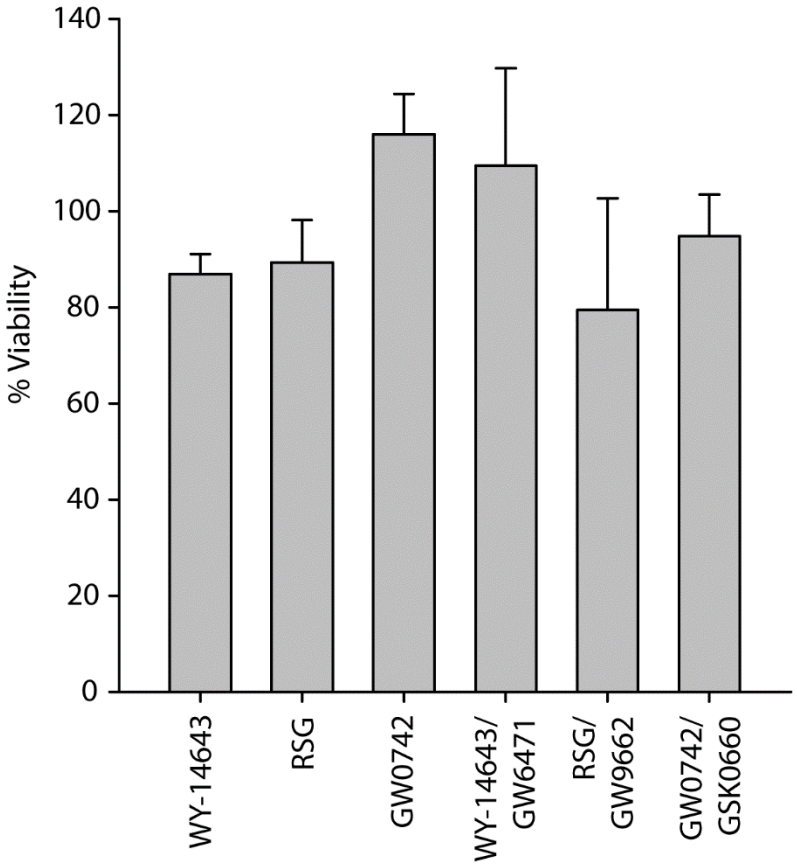

Fig. S4. Effect of PPAR agonists and antagonists on macrophage cell viability.

Sulforhodamine B (SRB) was used to assess cytotoxic effects of PPAR agonists (PPARα, WY-14643; PPARγ, rosiglitazone (RSG); PPARδ, GW0742) or PPAR agonists and antagonists (PPARα, GW6471; PPARγ, GW9662; PPARδ, GSK0660). The agonists and antagonists were incubated with freshly isolated murine peritoneal macrophages at 2x their respective EC50 or IC50 (see Table S9). Percent control growth is expressed as % viability and is a ratio of the amount of growth that occurred with treatment over the amount of growth that occurred in media. One hundred percent indicates no differences in cell growth between treatment and

media, whereas values below 100% indicate that growth was impaired with treatment. Data are expressed as mean ± SEM of 3-7 mice per condition

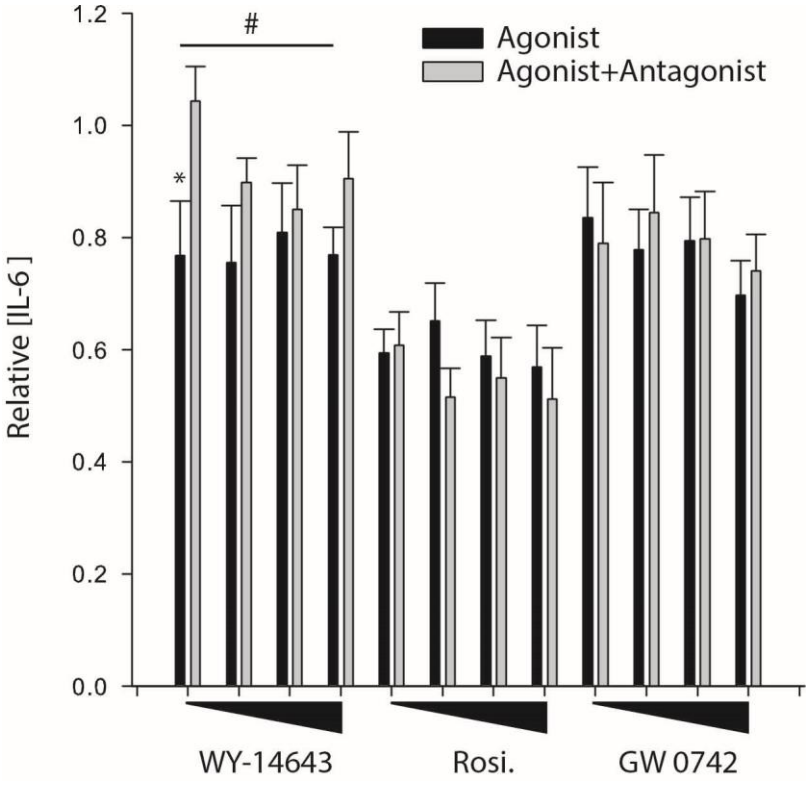

Fig. S5. Suppression of IL-6 in LPS-stimulated macrophages is achieved through activation of PPARα and reversed by addition of a PPARα antagonist.

Murine peritoneal macrophages were incubated with peroxisome proliferator-activated receptor (PPAR) α antagonist (GW 6471), PPARγ antagonist (GW 9662), PPARδ antagonist (GSK 0660), or Dulbecco's Modified Eagle Medium (DMEM)/F-12. After a 1-h incubation, the cells were treated with the complementary agonist (PPARα: WY-14643, PPARγ: rosiglitazone; Rosi., PPARδ: GW 0742). For each agonist, four concentrations were assayed, 1x, 2x, 5x, and 10x the half-maximal effective concentration (EC_{50}). The immune response was measured as the

concentration of interleukin (IL) 6 in the cell supernatant relative to vehicle controls. #$p < 0.05$ main effect of agonist + antagonist condition relative to agonist alone condition in a multifactor ANOVA. *$p < 0.05$, Fisher's least significant difference (LSD), pairwise comparison relative to antagonist-treated cells.